

# Surface Scattering & Spectroscopy

Tai C. Chiang

Department of Physics, University of Illinois at Urbana-Champaign

---

## *Outline*

*Brief review of x-ray diffraction from solids*

*Surfaces – relaxation & reconstruction; roughness; adsorbates*

*Truncation rods & fractional-order spots/rods; structure determination*

*Thin films – reflectivity and fractional-order rods*

*Growth issues, roughness, nanostructures*

*XPS (x-ray photoelectron spectroscopy)*

*Auger spectroscopy*

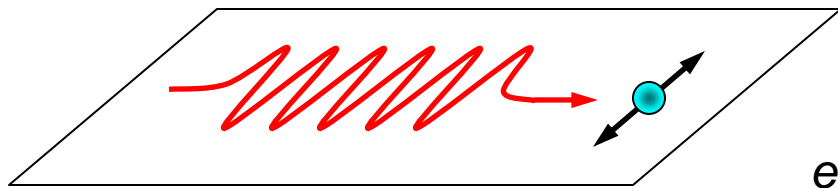
# Brief Review of the Basics of X-Ray Diffraction/Scattering

X-ray interaction with charged particles ( $\propto 1/m$ ):

Dominated by electrons; nuclei ignored

$$H = \frac{1}{2m} \left( \mathbf{p} - \frac{q}{c} \mathbf{A} \right)^2 + V(\mathbf{r})$$

**Scattering by a single electron** – electron oscillates in incident field and radiates with a dipole pattern – Thomson formula



$$\frac{d\sigma}{d\Omega} = r_0^2 P$$

$$r_0 = \frac{e^2}{mc^2} = 2.82 \times 10^{-5} \text{ \AA} = \text{Thomson scattering length}$$

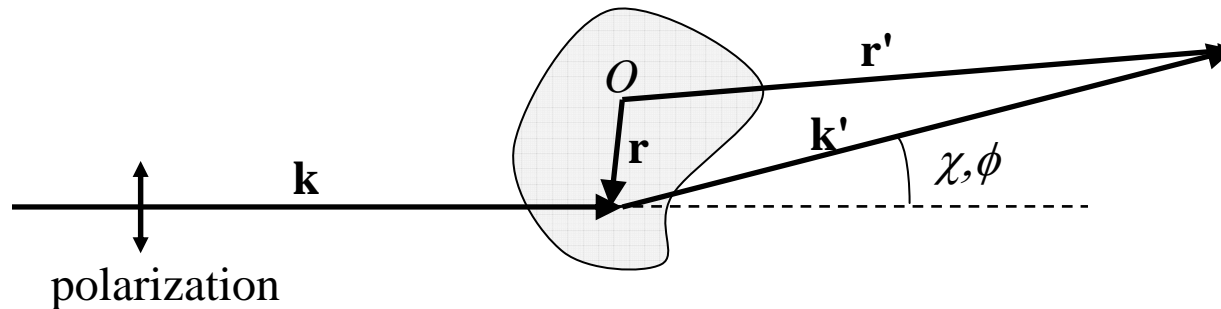
Weak process, single scattering ~OK, kinematic theory OK

Polarization factor:  $P = \sin^2 \chi + \cos^2 \chi \cos^2 \phi$

$\phi$  = scattering angle       $\chi$  = angle between incident polarization & scattering plane

$P = (1 + \cos^2 \phi) / 2$       for unpolarized sources.

## Scattering by an object (many electrons) – coherent sum of amplitudes



$A$  = total scattering amplitude at  $\mathbf{r}'$  (detector)  $\propto \int$  (amplitude of incident plane wave)  $\times$  (number of electrons in  $d^3r$ )  $\times$  (amplitude of scattered spherical wave at  $\mathbf{r}'$ )

$$A \propto \int_V (e^{i\mathbf{k}\cdot\mathbf{r}}) (n(\mathbf{r}) d^3r) \left( \frac{e^{ik'|\mathbf{r}'-\mathbf{r}|}}{|\mathbf{r}'-\mathbf{r}|} g(\chi, \phi) \right)$$

Far field approximation:  $|\mathbf{r}'-\mathbf{r}| \sim r'$   $e^{ik'|\mathbf{r}'-\mathbf{r}|} = e^{i\mathbf{k}'\cdot(\mathbf{r}'-\mathbf{r})}$

$$A \propto \frac{g}{r'} \int n(\mathbf{r}) e^{i\mathbf{k}\cdot\mathbf{r}} e^{i\mathbf{k}'\cdot(\mathbf{r}'-\mathbf{r})} d^3r = \frac{g}{r'} e^{i\mathbf{k}'\cdot\mathbf{r}'} \int d^3r n(\mathbf{r}) e^{-i\Delta\mathbf{k}\cdot\mathbf{r}}$$

$\mathbf{Q} \equiv \Delta\mathbf{k} = \mathbf{k}' - \mathbf{k}$  = scattering wavevector (momentum transfer)

$$I \propto P \left| \int d^3r n(\mathbf{r}) e^{-i\mathbf{Q}\cdot\mathbf{r}} \right|^2$$

$P$  = polarization factor

Intensity  $\propto P \times$  Absolute square of the Fourier transform of electron density

For a crystal: 
$$n(\mathbf{r}) = \sum_{\mathbf{R}, j} n_j(\mathbf{r} - \mathbf{R} - \boldsymbol{\tau}_j - \mathbf{u}_j(\mathbf{R}))$$

$\mathbf{R}$  = lattice vector

$\boldsymbol{\tau}_j$  = position of  $j$ -th atom in unit cell

$n_j$  = atomic electronic density

$\mathbf{u}$  = thermal vibration (ignore for now)

$$\begin{aligned} I &\propto P \left| \int d\mathbf{r} \sum_{\mathbf{R}, j} n_j(\mathbf{r} - \mathbf{R} - \boldsymbol{\tau}_j) e^{-i\mathbf{Q}\cdot\mathbf{r}} \right|^2 \\ &= P \left| \sum_{\mathbf{R}, j} e^{-i\mathbf{Q}\cdot\mathbf{R} - i\mathbf{Q}\cdot\boldsymbol{\tau}_j} \int d(\mathbf{r} - \mathbf{R} - \boldsymbol{\tau}_j) \sum_{\mathbf{R}, j} n_j(\mathbf{r} - \mathbf{R} - \boldsymbol{\tau}_j) e^{-i\mathbf{Q}\cdot(\mathbf{r} - \mathbf{R} - \boldsymbol{\tau}_j)} \right|^2 \\ &= P \left| \sum_{\mathbf{R}, j} e^{-i\mathbf{Q}\cdot\mathbf{R} - i\mathbf{Q}\cdot\boldsymbol{\tau}_j} f_j \right|^2 = P \left| \sum_j e^{-i\mathbf{Q}\cdot\boldsymbol{\tau}_j} f_j \right|^2 \left| \sum_{\mathbf{R}} e^{-i\mathbf{Q}\cdot\mathbf{R}} \right|^2 \end{aligned}$$

$f_j(\mathbf{Q})$  = Fourier transform of atomic electron density = atomic form factor

$$\sum_j e^{-i\mathbf{Q}\cdot\boldsymbol{\tau}_j} f_j = \text{unit cell structure factor} \quad S(\mathbf{Q}) \equiv \sum_{\mathbf{R}} e^{-i\mathbf{Q}\cdot\mathbf{R}} = \text{lattice sum}$$

Thermal vibration  $\rightarrow$  reduction of amplitude by the Debye Waller factor  
 $\exp(-W)$  + weak thermal diffuse scattering (scattering by phonons; ignored)

Intensity  $\propto$  (Debye-Waller)  $\times$  (polarization)  $\times$  (atomic form factor or unit cell structure factor, squared)  $\times$  (lattice sum squared)

For an ideal 3D crystal:

$$\sum_{\mathbf{R}} e^{-i\mathbf{Q}\cdot\mathbf{R}} = N \sum_{\mathbf{G}} \delta_{\mathbf{Q},\mathbf{G}} \quad \mathbf{G} = \text{reciprocal lattice vector} \quad N = \# \text{ unit cells in system}$$

**Laue condition:** diffraction occurs at  $\mathbf{Q} = \mathbf{G}$  (Bragg peaks - delta functions)

For surface scattering, we are primarily interested in the lattice sum and structure factor. Debye-Waller, polarization, and atomic form factors are slowly varying functions of  $\mathbf{Q}$  (available from calculations or tables). Data are often normalized by these factors before analysis.

Assume that data normalization has been carried out (unless otherwise specified).

For surfaces & films, the lattice sum is truncated or finite along  $z$ . One obtains delta functions in the  $xy$  plane only. Diffraction along  $z$  has a broadened profile (rods), which carries structural information.

## Common Surface Effects

---

**Relaxation** – atomic layer spacings near a surface might be modified due to atomic force imbalance; often oscillatory due to quantum effects

**Reconstruction** – near-surface atomic positions might be modified; examples: Si(111)-(2x1) metastable face obtained by cleavage, Si(111)-(7x7) after annealing, Si(100)-(2x1), Ge(100)-(2x1), Ge(111)-c(2x8)

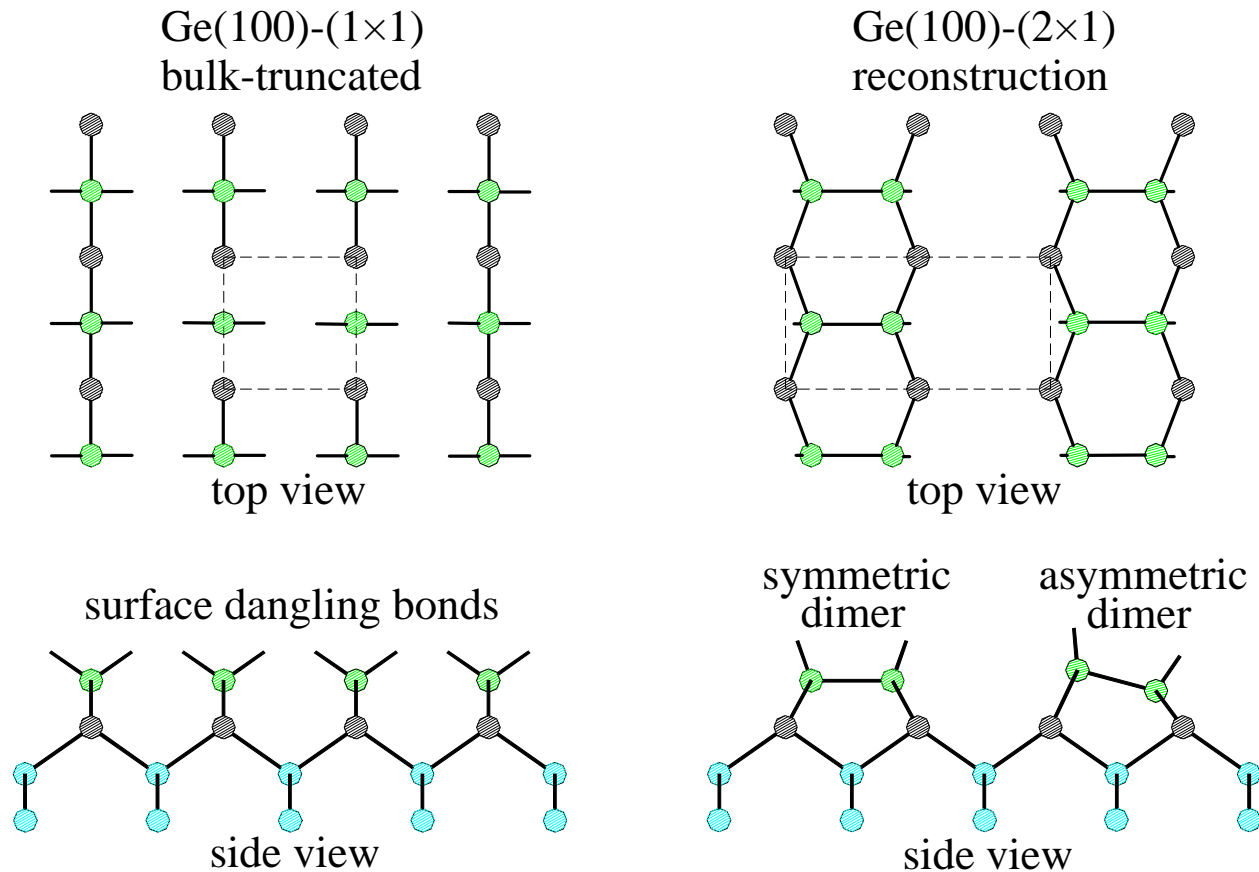
Driven by energy minimization: reducing the number of dangling bonds by rebonding, balanced by increase in strain energy.

**Roughness** – nothing is perfect; entropy effects and energetics (step generation and bunching; low-energy facet formation; quantum size effects; ...); kinetics (system has not had a chance to settle down).

**Self-assembled nanostructures** – resulting from electronic effects & strain; could be viewed as reconstruction at large length scales.

These structural features can be characterized by x-ray diffraction.

## Example: Ge(100)-(2x1) or c(4x2)



**Dimer** formation reduces the number of dangling bonds.

At room temperature, the structure is (2x1). At low T, the structure is c(4x2), with the dimers alternately asymmetrically oriented (to minimize the free energy).

# X-ray Diffraction Patterns

In 3D, the pattern is basically the reciprocal lattice.

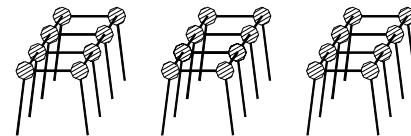
$$S = \sum_{\mathbf{R}} e^{-i\mathbf{Q}\cdot\mathbf{R}} = N \sum_{\mathbf{G}} \delta_{\mathbf{Q},\mathbf{G}}$$

For a 2D monolayer, the pattern is the 2D reciprocal lattice, or a 2D array of rods (no  $Q_z$  dependence)

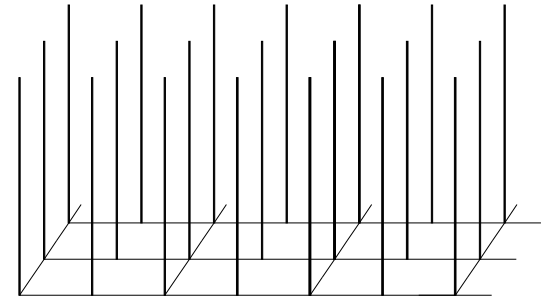
For a truncated surface, the pattern is a set of **truncation rods**.

For reconstructed surfaces, there are superlattice rods (**fractional-order rods**).

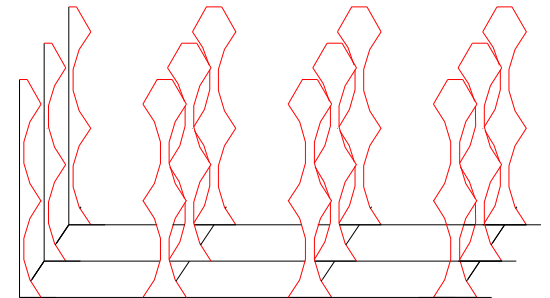
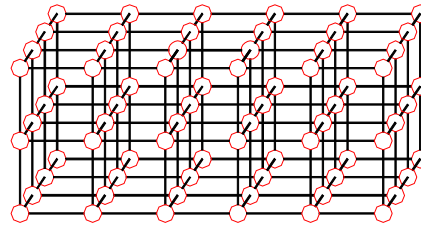
Real Space



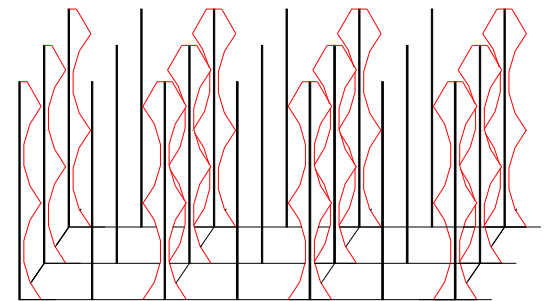
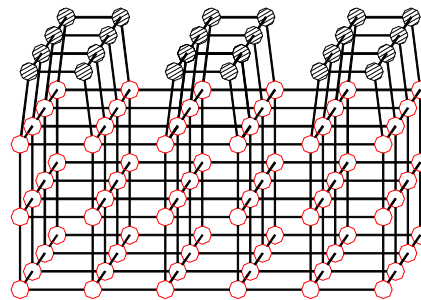
Ideal (2×1) monolayer - 2-D Bragg rods



Ideal bulk-truncated crystal - Crystal truncation rods



Ideal (2×1) surface/interface reconstruction



## Truncation Rods

Consider an ideal truncated crystal with surface unit cell vectors  $\mathbf{a}_1$  &  $\mathbf{a}_2$ ;  $\mathbf{a}_3$  must be chosen along  $z$  in order to have  $\mathbf{b}_1$  and  $\mathbf{b}_2$  within the surface plane. The choices of  $\mathbf{a}_1$ ,  $\mathbf{a}_2$ , &  $\mathbf{a}_3$  are often different from the bulk case.

$$\mathbf{R} = n_1 \mathbf{a}_1 + n_2 \mathbf{a}_2 + n_3 \mathbf{a}_3 \quad \mathbf{Q} = Q_1 \mathbf{b}_1 + Q_2 \mathbf{b}_2 + Q_3 \mathbf{b}_3 \quad \mathbf{G} = h\mathbf{b}_1 + k\mathbf{b}_2 + l\mathbf{b}_3 \equiv (hkl)$$

$$S \equiv \sum_{\mathbf{R}} e^{-i\mathbf{Q} \cdot \mathbf{R}} = \sum_{n_1, n_2, n_3} \exp[-i2\pi(Q_1 n_1 + Q_2 n_2 + Q_3 n_3)]$$

$$= \left( N_1 \sum_h \delta_{Q_1, h} \right) \left( N_2 \sum_k \delta_{Q_2, k} \right) \left( \sum_{n_3=0}^{-\infty} \exp(-i2\pi Q_3 n_3) \right) \equiv S_1 S_2 S_3$$

$S_1$  &  $S_2$  are the same as those for infinite crystals. In reality, the sum  $S_3$  is over a finite number of layers due to x-ray absorption. We simulate this effect by adding a small imaginary part to  $Q_3$  (for damping).

$$S_3 = \sum_{n_3=0}^{-\infty} \exp[-i(2\pi Q_3 + i\varepsilon)n_3] = 1 + e^{i2\pi Q_3 - \varepsilon} + e^{i4\pi Q_3 - 2\varepsilon} + \dots = \frac{1}{1 - \exp[i(2\pi Q_3 + i\varepsilon)]}$$

A 1D sum of scattering amplitudes from the layers. Each successful layer has an additional phase shift of  $\exp(i2\pi Q_3)$  & an attenuation factor  $\exp(-\varepsilon)$ .

$$|S_3|^2 = \left| \frac{1}{1 - \exp(i2\pi Q_3) \exp(-\varepsilon)} \right|^2 = \frac{1}{1 + e^{-2\varepsilon} - 2e^{-\varepsilon} \cos(2\pi Q_3)} \xrightarrow{\varepsilon \rightarrow 0} \frac{1}{4 \sin^2(\pi Q_3)}$$

Peaks at  $Q_3 = \text{integers}$  (Bragg points); but the intensity is finite in-between.

$$I_{CTR} \equiv |S_3|^2 = \frac{1}{1 + e^{-2\varepsilon} - 2e^{-\varepsilon} \cos(2\pi Q_3)} \sim 1 \text{ away from Bragg points}$$

$$I_{CTR} = (1 - e^{-\varepsilon})^{-2} \simeq \varepsilon^{-2} \text{ at Bragg points} \sim (\text{number of layers probed})^2$$

**Truncation rods** at  $(hk)$  are  $\perp$  to the surface and go through diffraction peaks  $(hkl)$ . Determined experimentally by  $I$ -scans.

The intensities at points away from diffraction peaks are  $\sim$  the intensity of a single layer. Weak but detectable.

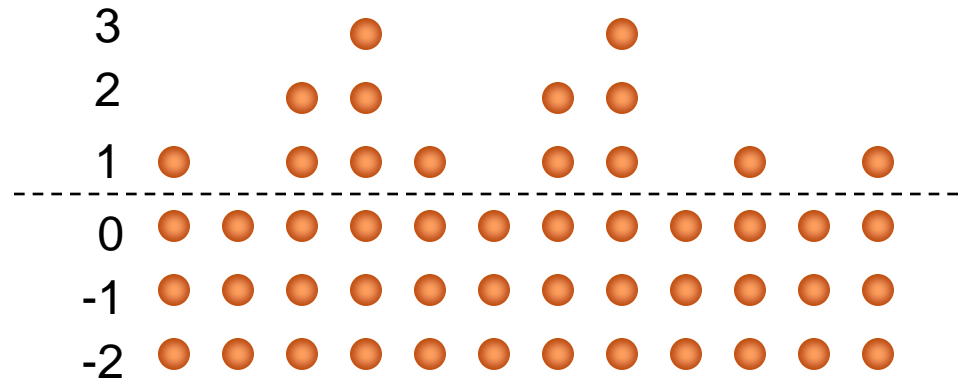
Rod profile is sensitive to surface relaxation/reconstruction.

**Logarithmic scales** are often used to show details between Bragg peaks (otherwise hard to see).

# Roughness

$$S_3 = \sum_{n_3=0}^{-\infty} \exp[-i(2\pi Q_3 + i\varepsilon)n_3] = 1 + e^{i2\pi Q_3 - \varepsilon} + e^{i4\pi Q_3 - 2\varepsilon} + \dots = \frac{1}{1 - \exp[i(2\pi Q_3 + i\varepsilon)]}$$

Simple model (exponential distribution) – Ignore absorption ( $\varepsilon$ ). Add additional layers on top: layer 1 **occupancy**  $\beta < 1$ , layer 2 occupancy  $\beta^2$ , etc.



$$S_3 = \frac{1}{1 - e^{i2\pi Q_3}} + \beta e^{-i2\pi Q_3} + \beta^2 e^{-i4\pi Q_3} + \dots = \frac{1}{1 - e^{i2\pi Q_3}} + \frac{\beta e^{-i2\pi Q_3}}{1 - \beta e^{-i2\pi Q_3}} = \frac{1}{1 - e^{i2\pi Q_3}} \frac{1 - \beta}{1 - \beta e^{-i2\pi Q_3}}$$

$$I_{\text{Rough}} \propto |S_3|^2$$

$$I_{\text{Rough}} = I_{\text{CTR}} \frac{(1-\beta)^2}{1+\beta^2 - 2\beta \cos(2\pi Q_3)}$$

Roughness factor has the same form as a truncation rod.

At **anti-Bragg points** ( $Q_3 = \text{half integers}$ , midway between Bragg peaks)

$$\frac{(1-\beta)^2}{1+\beta^2 - 2\beta \cos(2\pi Q_3)} = \frac{(1-\beta)^2}{(1+\beta)^2} < 1$$

At Bragg points ( $Q_3 = l = \text{integers}$ )

$$\frac{(1-\beta)^2}{1+\beta^2 - 2\beta \cos(2\pi Q_3)} = 1$$

Roughness tends to suppress the intensity between Bragg peaks.

## Numerical examples:

### log scale

Ideal truncated surface

$$F(Q) := \left( \left| \frac{1}{1 - \exp(i \cdot 2 \cdot \pi \cdot Q)} \right| \right)^2$$

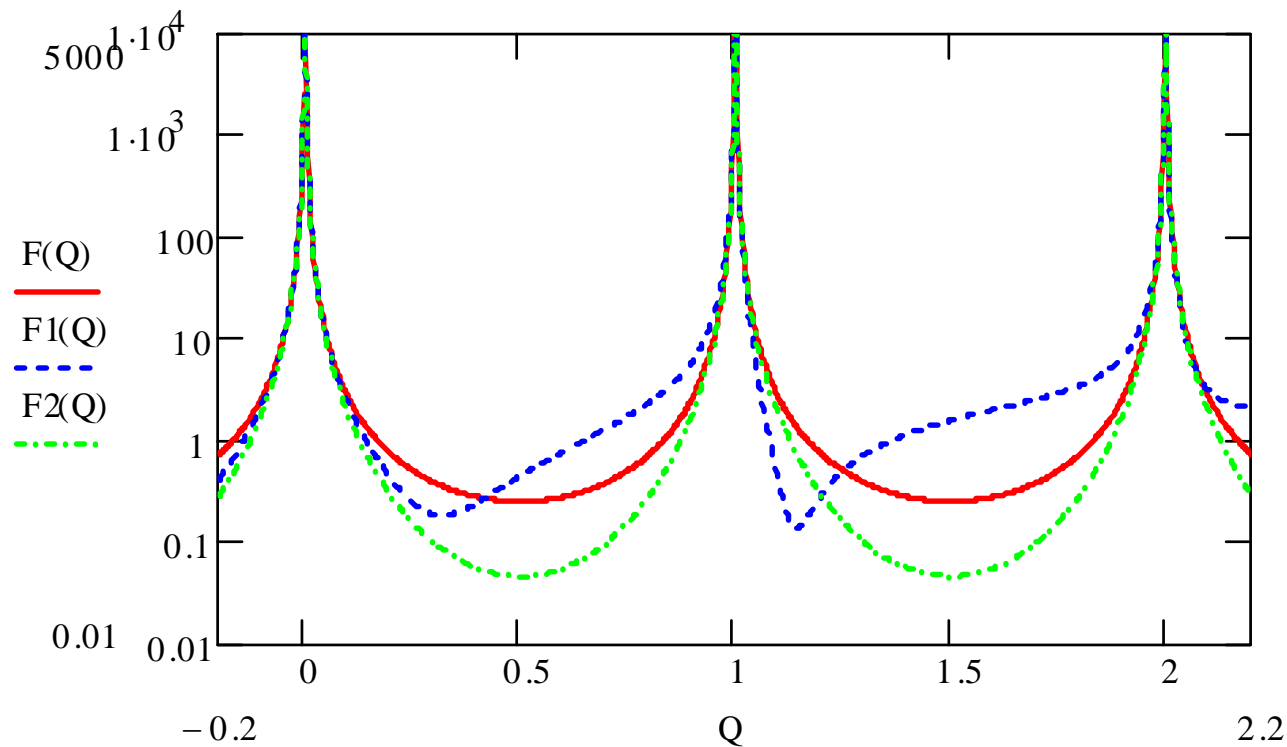
Top layer expanded by 20%

$$F1(Q) := \left( \left| \frac{1}{1 - \exp(i \cdot 2 \cdot \pi \cdot Q)} + \exp(-i \cdot 2 \cdot \pi \cdot Q \cdot 1.2) \right| \right)^2$$

Rough surface

$\beta := 0.4$

$$F2(Q) := \left( \left| \frac{1}{1 - \exp(i \cdot 2 \cdot \pi \cdot Q)} + \frac{\beta \cdot \exp(-i \cdot 2 \cdot \pi \cdot Q)}{1 - \beta \cdot \exp(-i \cdot 2 \cdot \pi \cdot Q)} \right| \right)^2$$



Rod scans  $\rightarrow$  structure (relaxation, etc.). Similar roughness model can be used to ~ describe **enhanced surface vibrations** (a larger Debye-Waller factor & a reduced scattering amplitude) and **disorder** (~ frozen phonons).

## (1x1) Adsorbates

Consider a (1x1) adsorbed layer, with atomic form factor  $f_a$ , on an ideal truncated substrate (atomic form factor  $f_s$ ), with the adsorbate-substrate spacing a factor  $x$  as large as the substrate layer spacing.

The lattice sum along  $z$  (with absorption ignored):

$$S = f_s (1 + e^{i2\pi Q_3} + e^{i4\pi Q_3} + \dots) + f_a e^{-2\pi x Q_3} = \frac{f_s}{1 - e^{i2\pi Q_3}} + f_a e^{-2\pi x Q_3}$$

$$I \propto |S|^2$$

The rod profile is sensitive to  $x$ , which is often the quantity of interest and can be deduced from fitting.

More complicated adsorbate systems can be analyzed similarly.

# Reconstructed Surfaces & Fractional-Order Rods

Recall that the intensity is determined by polarization factor, the unit cell structure factor, and the lattice sum.

$$I \propto P \left| \sum_{\mathbf{R}, j} e^{-i\mathbf{Q}\cdot\mathbf{R} - i\mathbf{Q}\cdot\mathbf{T}_j} f_j \right|^2 = P \left| \left( \sum_j e^{-i\mathbf{Q}\cdot\mathbf{T}_j} f_j \right) \left( \sum_{\mathbf{R}} e^{-i\mathbf{Q}\cdot\mathbf{R}} \right) \right|^2$$

With reconstructed surfaces, such as (2x1) or (7x7):

1. Choose  $\mathbf{a}_1$  and  $\mathbf{a}_2$  based on the supercell;  $\mathbf{a}_3$  along  $z$ .
2. Construct lattice sum for an ideal truncated substrate; there will be spurious superlattice (fractional order) rods that should not exist.
3. The supercell structure factor suppresses the spurious superlattice rods for the ideal (1x1) case (forbidden rods).
4. Add contributions from distorted substrate layers and adlayers on top, which give rise to observable fractional-order rods.
5. Take data along as many rods as you can; fit the data to get structure.

# Surface Crystallography

---

Ideally, one wants a 3D intensity map (possible with CCD and rapid rocking) – k-space mapping

In practice, one is often limited to:

(1) in-plane intensity map (a cut at small  $Q_3$  in  $k$  space with a grazing geometry to enhance surface sensitivity)

(2) Rod scans (**ridge scans** or a set of **rocking curves**) –

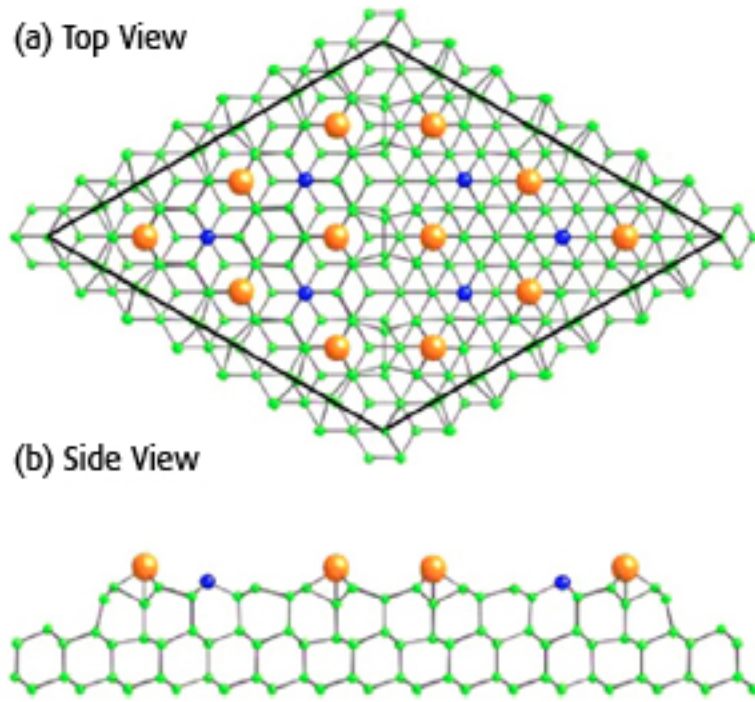
(00) rod ( $h = k = 0$ ), or **reflectivity** scan, is sensitive to vertical stacking, but insensitive to in-plane atomic positions.

( $hk$ ) rods are sensitive to both vertical and in-plane information.

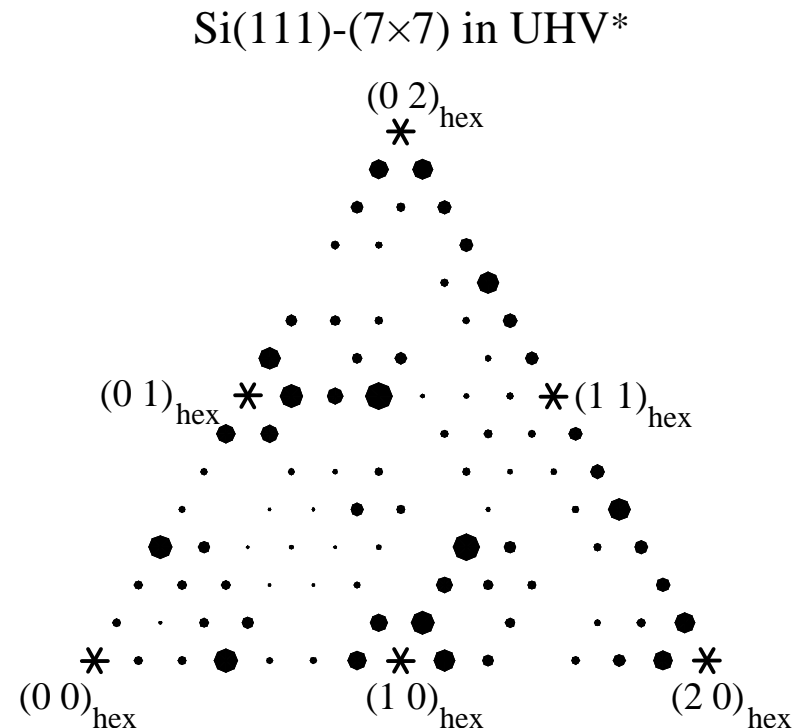
Fractional order rods are sensitive to reconstruction.

Other techniques of interest: Patterson analysis, difference Fourier maps, ..

# Example – Si(111)-(7x7) in UHV



From Omicron Nanotechnology



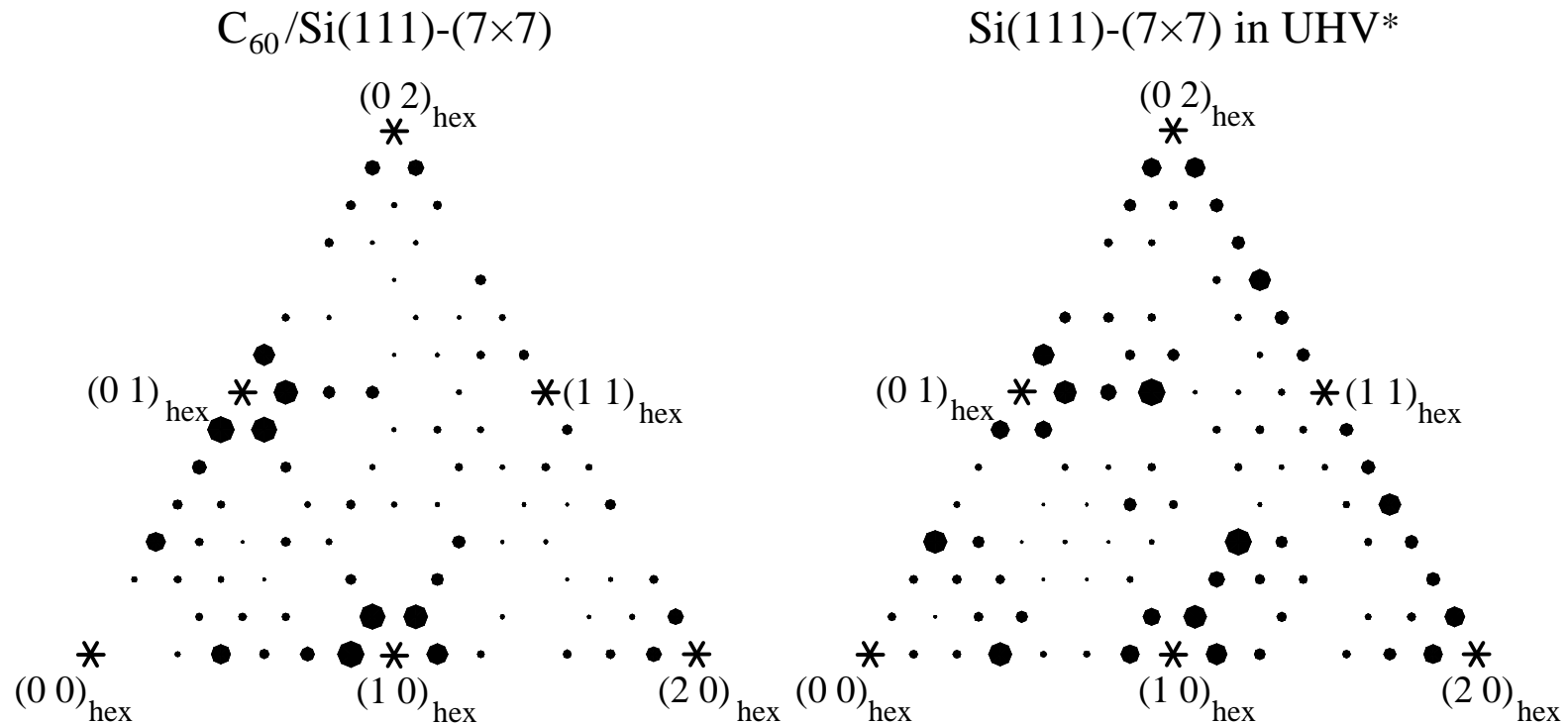
\*Courtesy of I. K. Robinson  
(Phys. Rev. B **33**, 7013 (1986))

(7x7) features include dimers, adatoms, & stacking faults (DAS model).

X-ray data: in-plane intensity map ( $h, k, Q_3$ ), with  $Q_3$  small (grazing geometry);  $h$  &  $k = 0, 1/7, 2/7, \dots$  (**integer & fraction-order spots**)

Structural information can be deduced from model fitting.

# Example – Si(111)-(7x7) Preserved Under C<sub>60</sub>



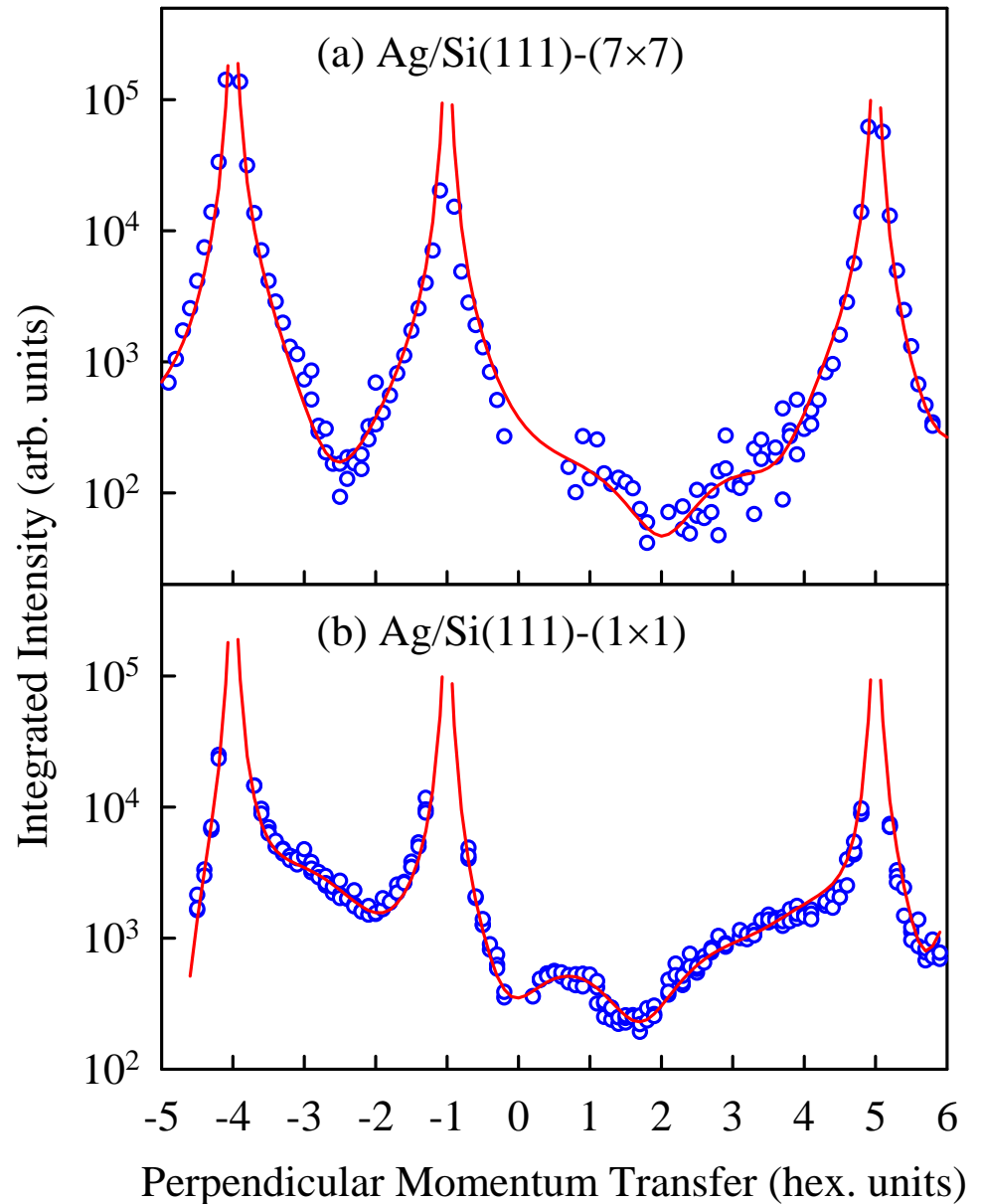
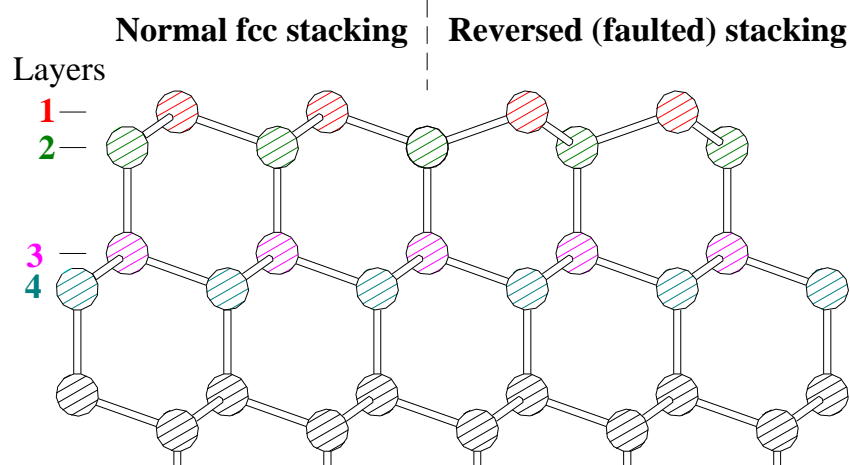
\*Courtesy of I. K. Robinson  
(Phys. Rev. B **33**, 7013 (1986))

The  $(7\times 7)$  features are largely intact (preserved) under a layer of  $C_{60}$ .  
The minor changes in structure can be deduced from the x-ray data.

# Example: Si(111)-(7x7) Capped by Ag & Its Transition to (1x1)

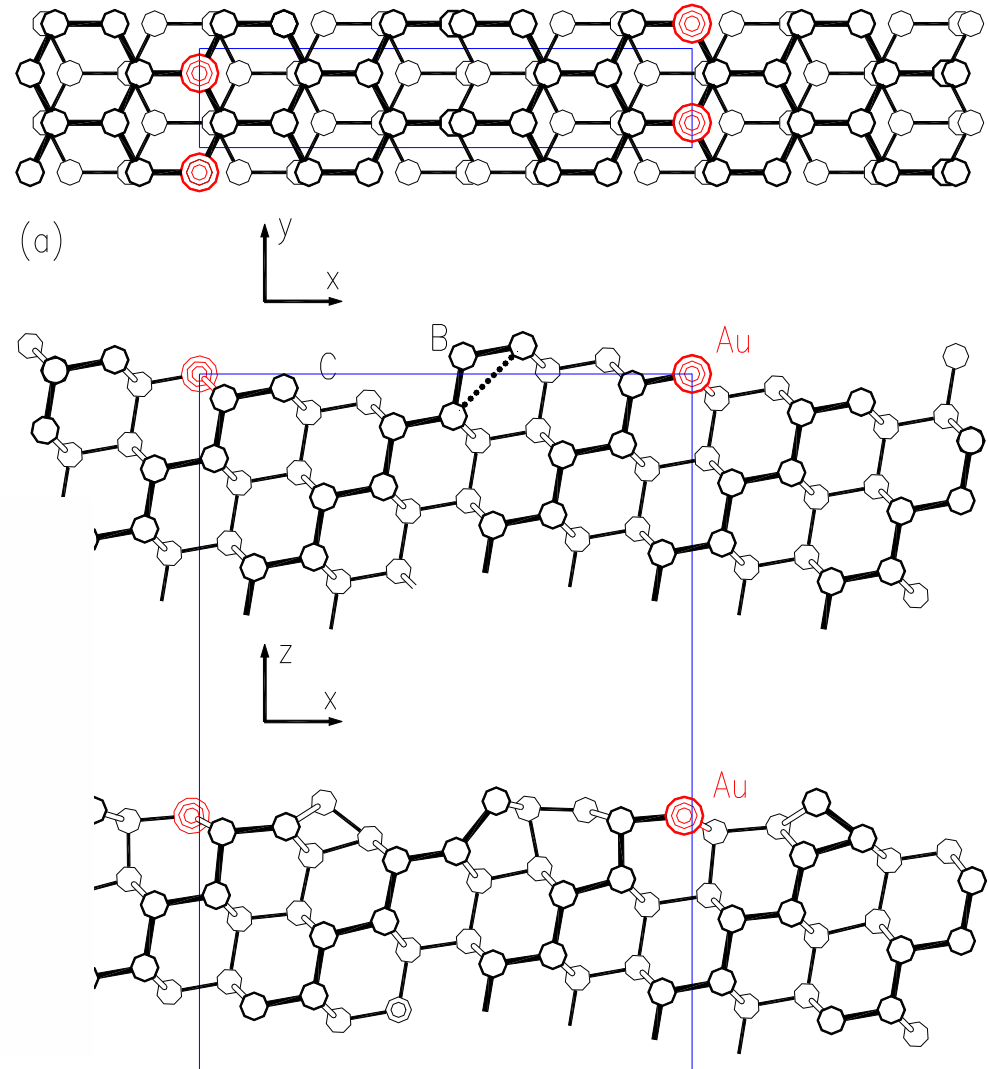
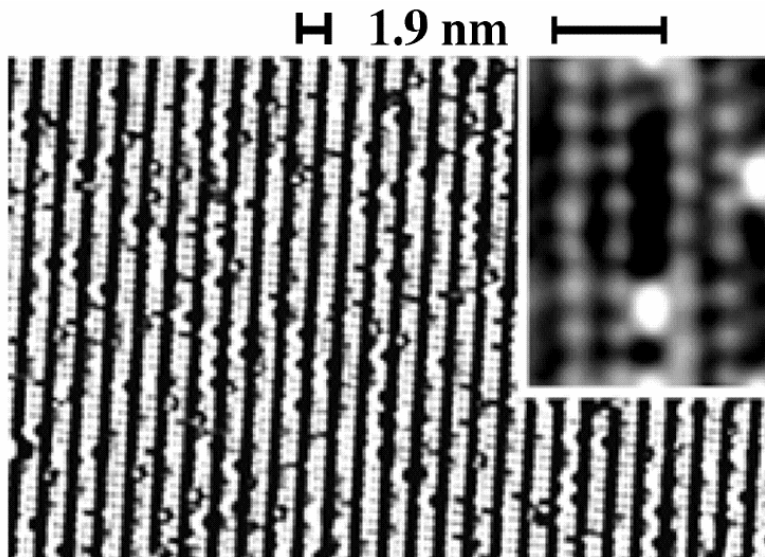
Si(111)-(7x7) capped by Ag at room temperature retains the (7x7) symmetry. The stacking fault feature is retained, but the adatom feature is gone.

Upon annealing to ~250 C, the interface structure becomes (1x1). Si (10/) rod scans show that the stacking fault is removed.

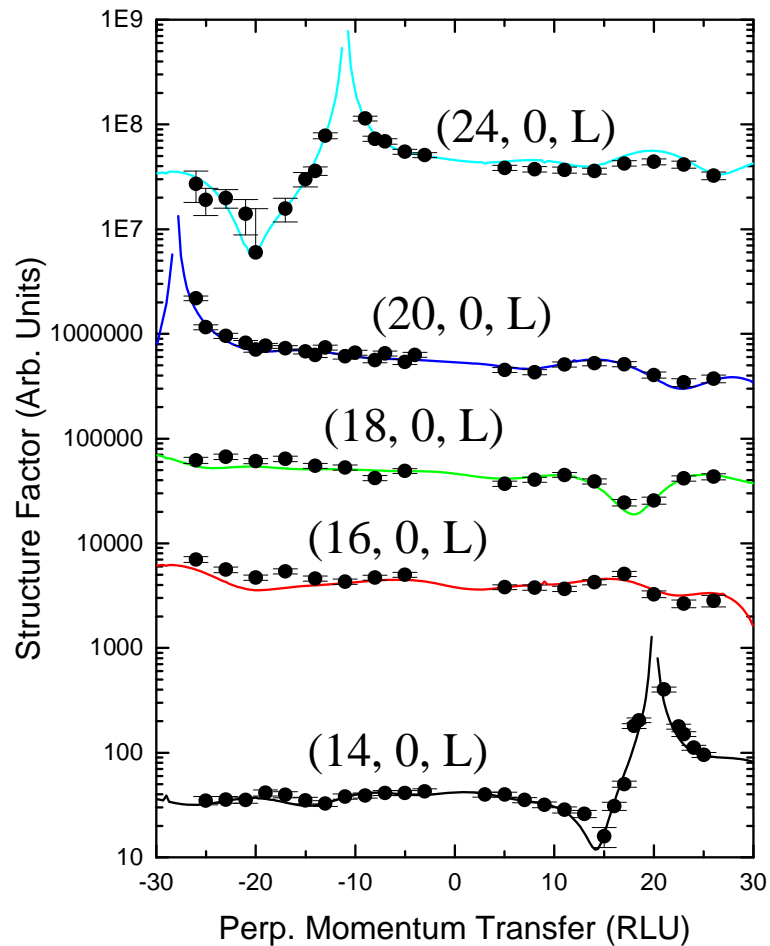
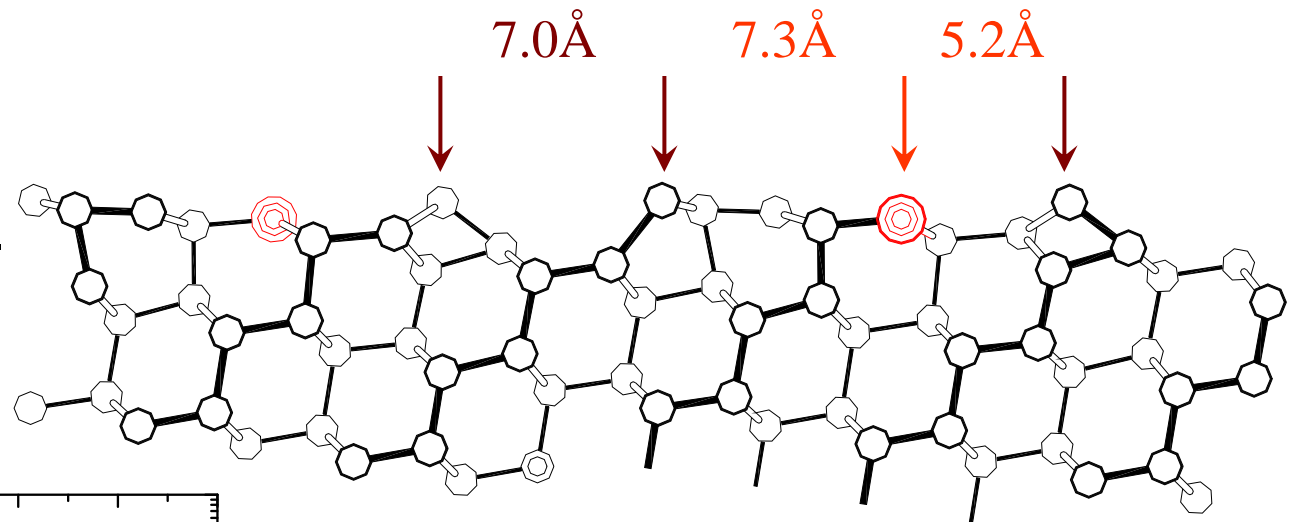


# Example: Si(557)-Au “Atomic Wires” (Ian K. Robinson)

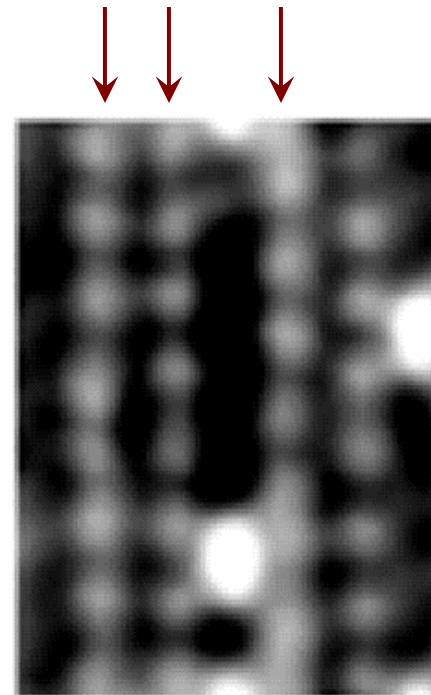
A periodic array of single steps stabilized by 0.2 monolayer of Au based on STM. Unusual (controversial) electronic structure based on photoemission. Long debate about atomic structure.



A tour de force of surface crystallography by truncation rod scans and Patterson analysis.



$7.3 \pm 0.7\text{\AA}$



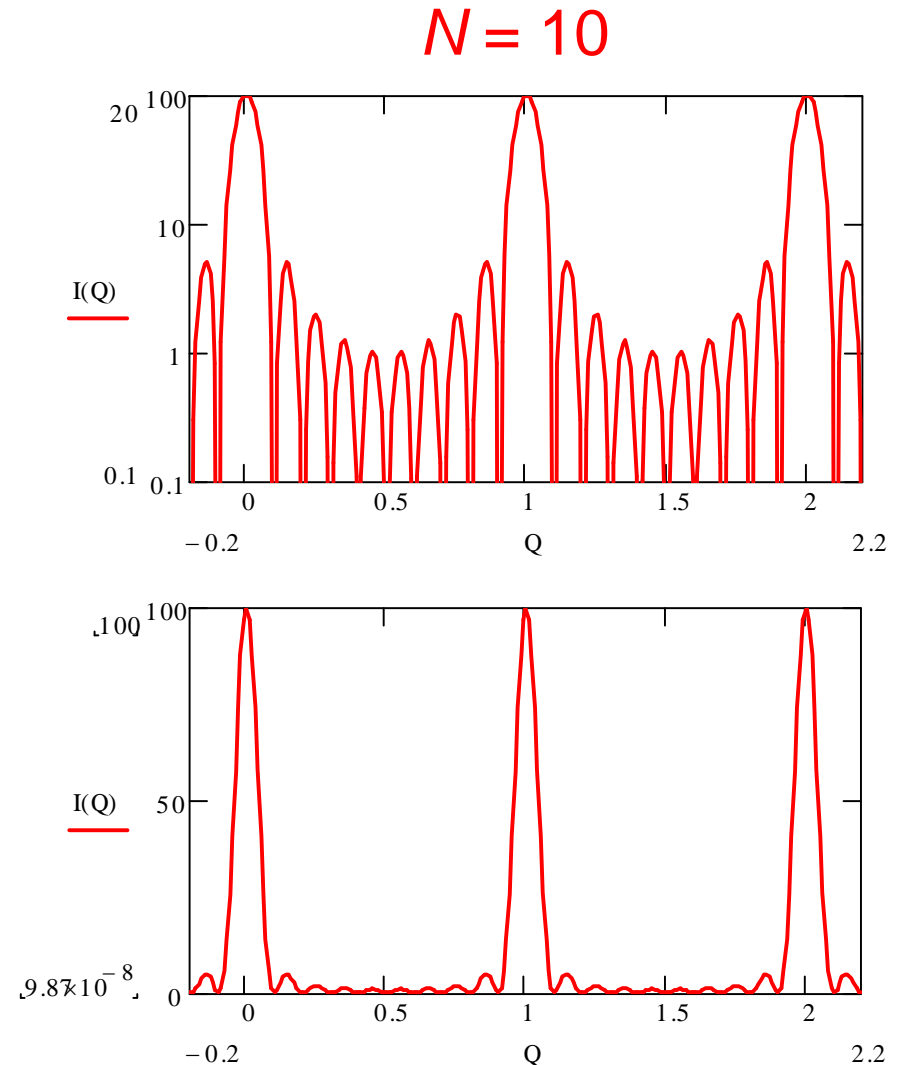
# Films & Growth

An ideal film of  $N$  atomic layers: the lattice sum for each rod becomes finite – an  **$N$ -slit diffraction pattern**.

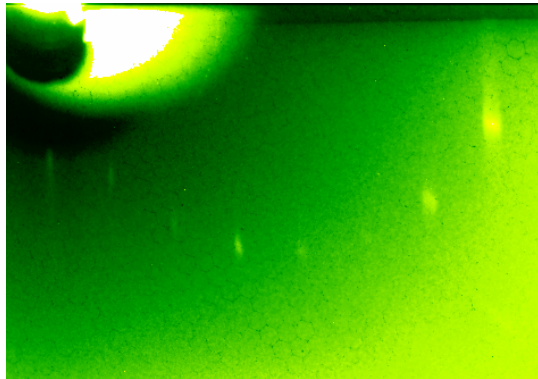
$$S_3 = \sum_{n_3=0}^{-N+1} \exp(-i2\pi Q_3 n_3) = \frac{1 - \exp(iN2\pi Q_3)}{1 - \exp(i2\pi Q_3)}$$

The Bragg peaks are broadened by the finite size (not a delta function any more). There are 8, or  $N - 2$ , satellite peaks between two neighboring Bragg peaks ( $N$  peaks including the two end Bragg peaks).

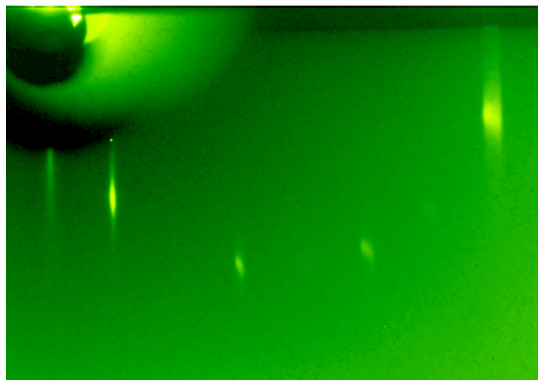
Peak counting yields the film thickness. Layer relaxation or reconstruction affects the profile.



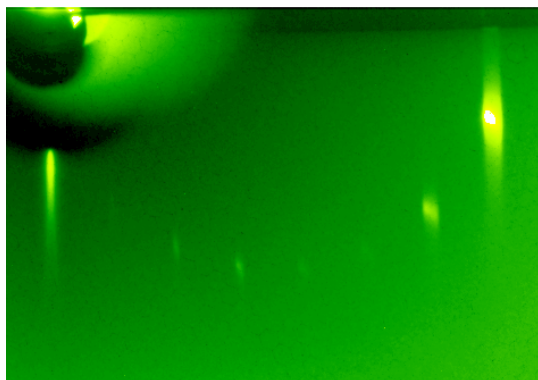
# Example: Pb Growth on Si(111)-(7x7)



Si(111)-(7x7)

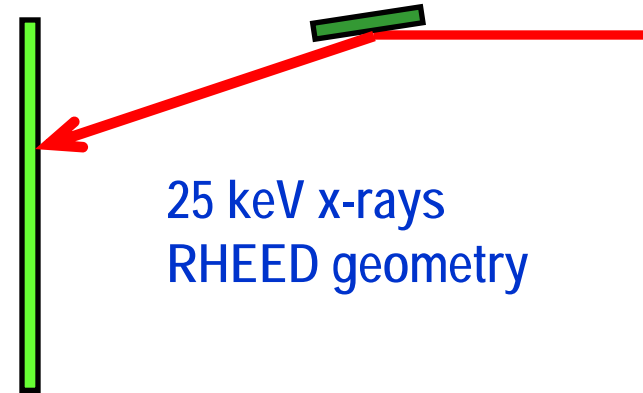


+ 0.5 ML Pb

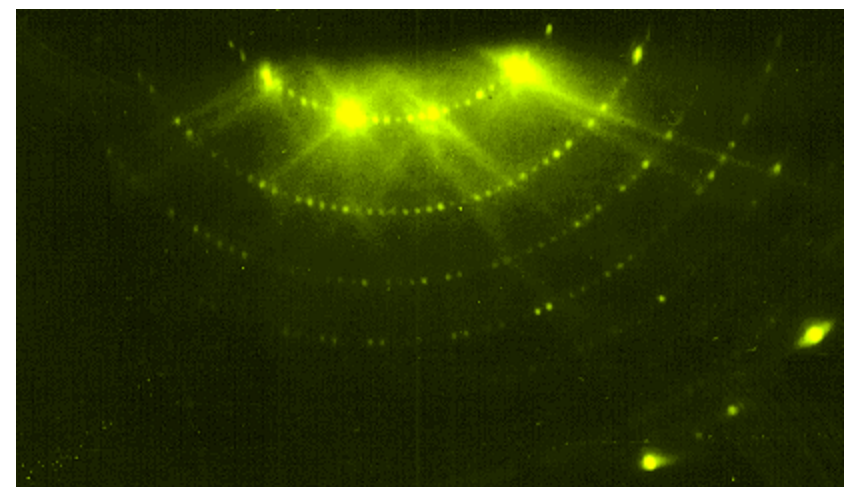


+ 1.2 ML Pb

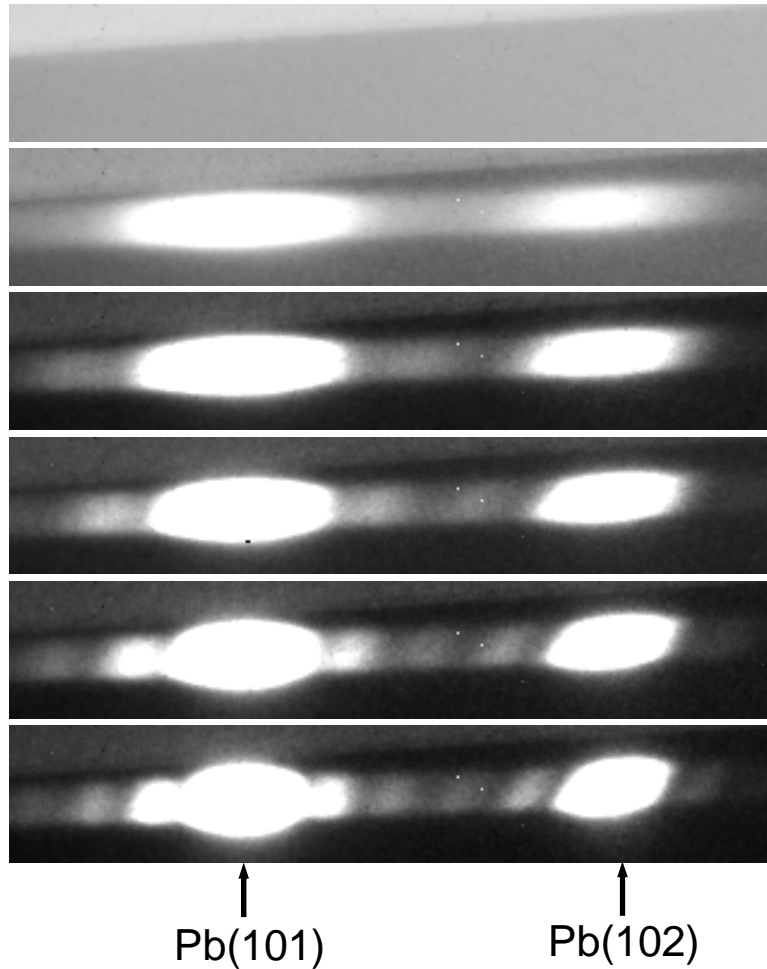
more intense  
(7x7); a  
commensurate  
wetting layer



RHEED 10 keV Si(111)-(7x7)



# Pb (10L) Rod Profile during Deposition at 180 K



$t = 379$  s

1044 s

1811 s

2527 s

3345 s

4368 s

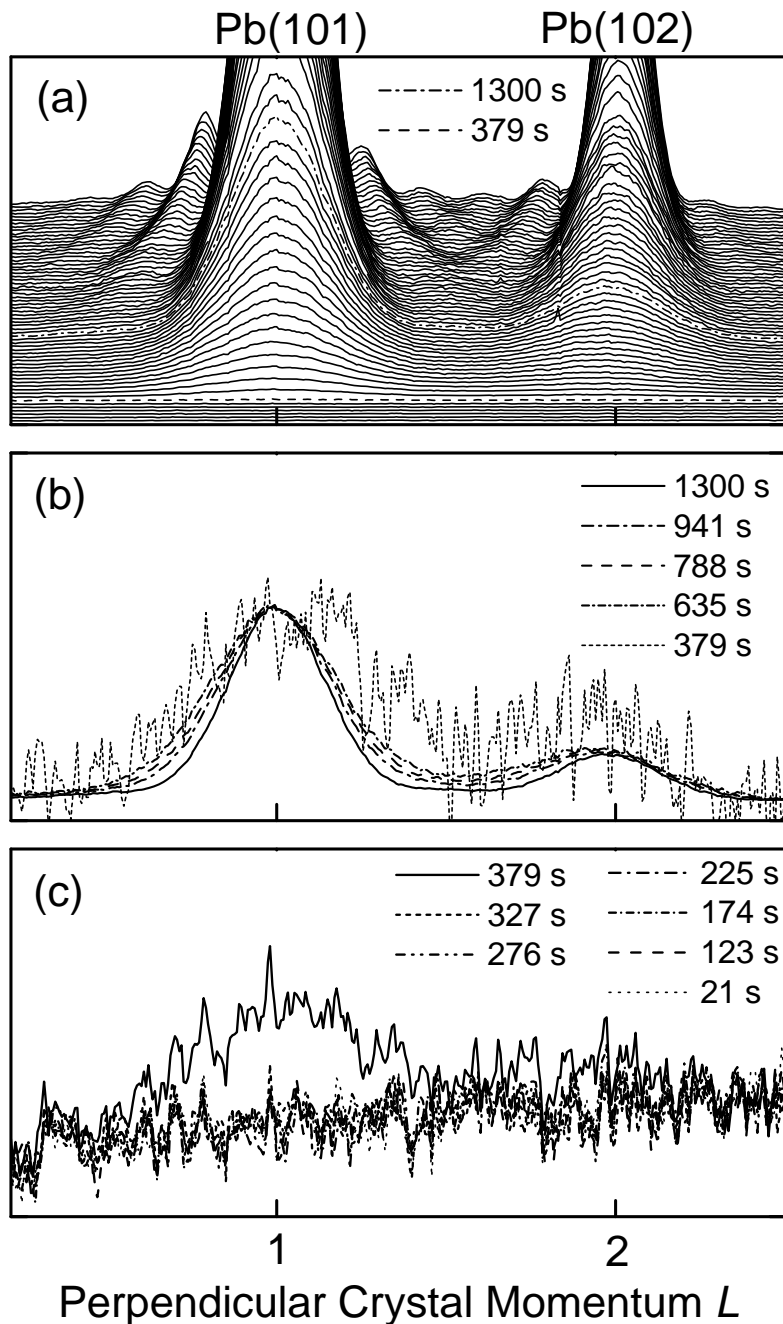
19 ML =  $6 \times 3 + 1$

Mosaic spread broadens rods & allows a length of rod to be captured by CCD (no need to do rocking curves)

Development of Pb Bragg peaks & multilayer interference peaks

Each "layer" is 3 atomic layers (ABC stacking for fcc);  $\mathbf{a}_3$  must be  $\perp$  surface.

Intensities (arb. units)

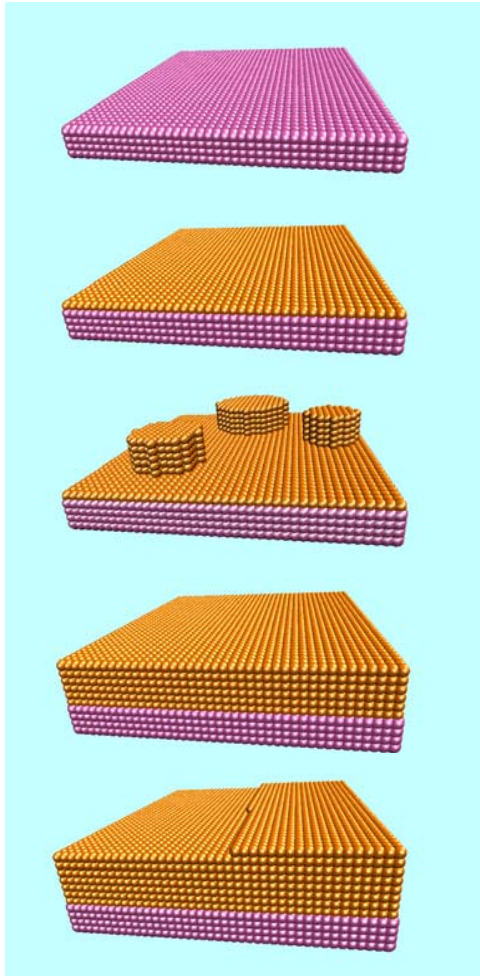


Beyond ~6 ML, smooth evolution of multilayer satellite peaks implies layer-by-layer growth

1.5 – 6 ML, constant profile; islands of height ~6 ML (from fitting) growing laterally to fill surface

Sharp onset of Pb Bragg peaks at ~350 s (1.5 ML) – formation of Pb islands

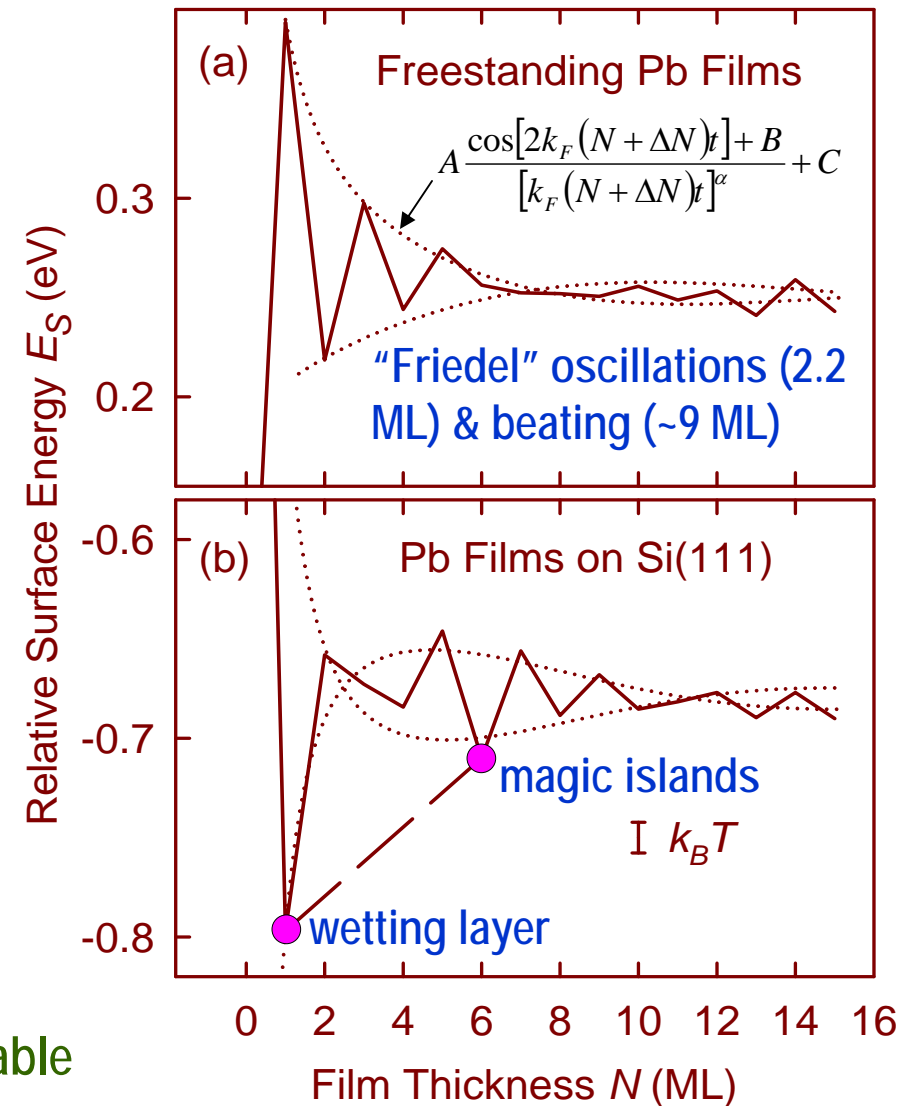
# Quantum Phase Separation Caused by Electronic Effects



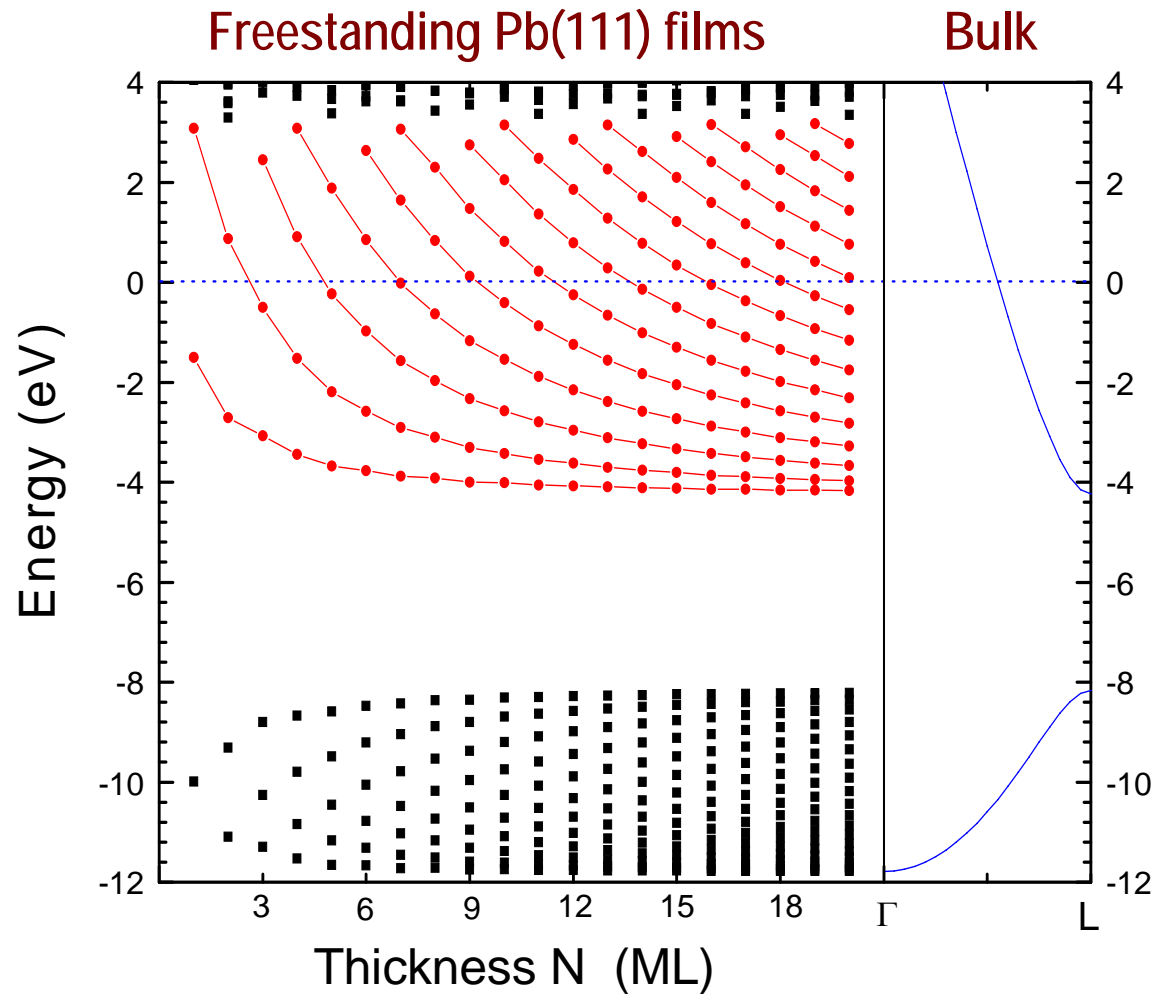
Quantum oscillations: 2.2 ML

Global energy landscape: 1 & 6 ML most stable

## First-principles calculation



# Quantum Well States & Quantum Oscillations



Fermi level crossing of subbands - sharp changes in electronic density and properties

Period of quantum oscillations:

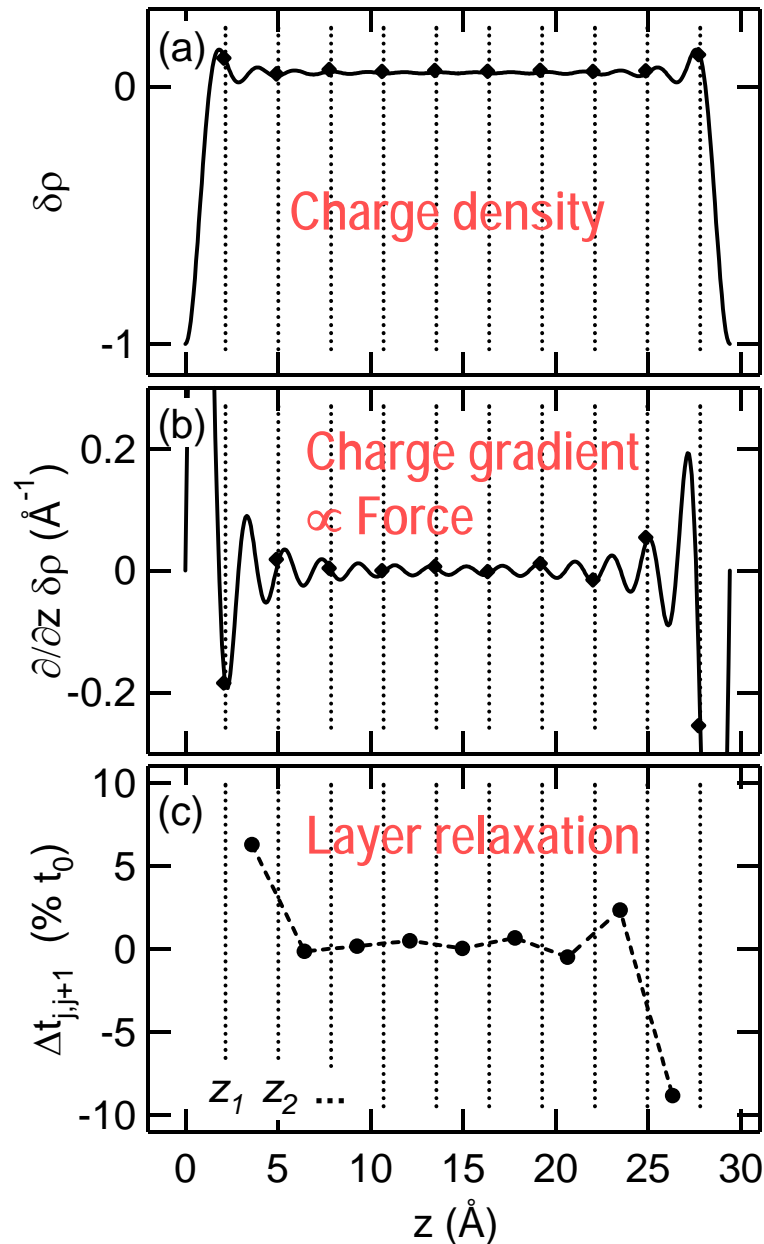
$$2kd + \Phi = 2n\pi$$

At the Fermi level,

$$2k_F \Delta d = 2\pi \text{ for } \Delta n = 1$$

$$\Delta d = \frac{\pi}{k_F} = \frac{\lambda_F}{2} = \boxed{2.2 \text{ ML}}$$

## Another Quantum Size Effect: Charge Oscillations in Real Space



Charge density (for free electrons in a box) shows Friedel-like damped oscillations with period 2.2 ML in Pb(111) films ( $2k_F$  effect).

Charge gradient at each atomic plane (electric field) causes position shift (atomic layer relaxation) – 2.2 ML oscillations

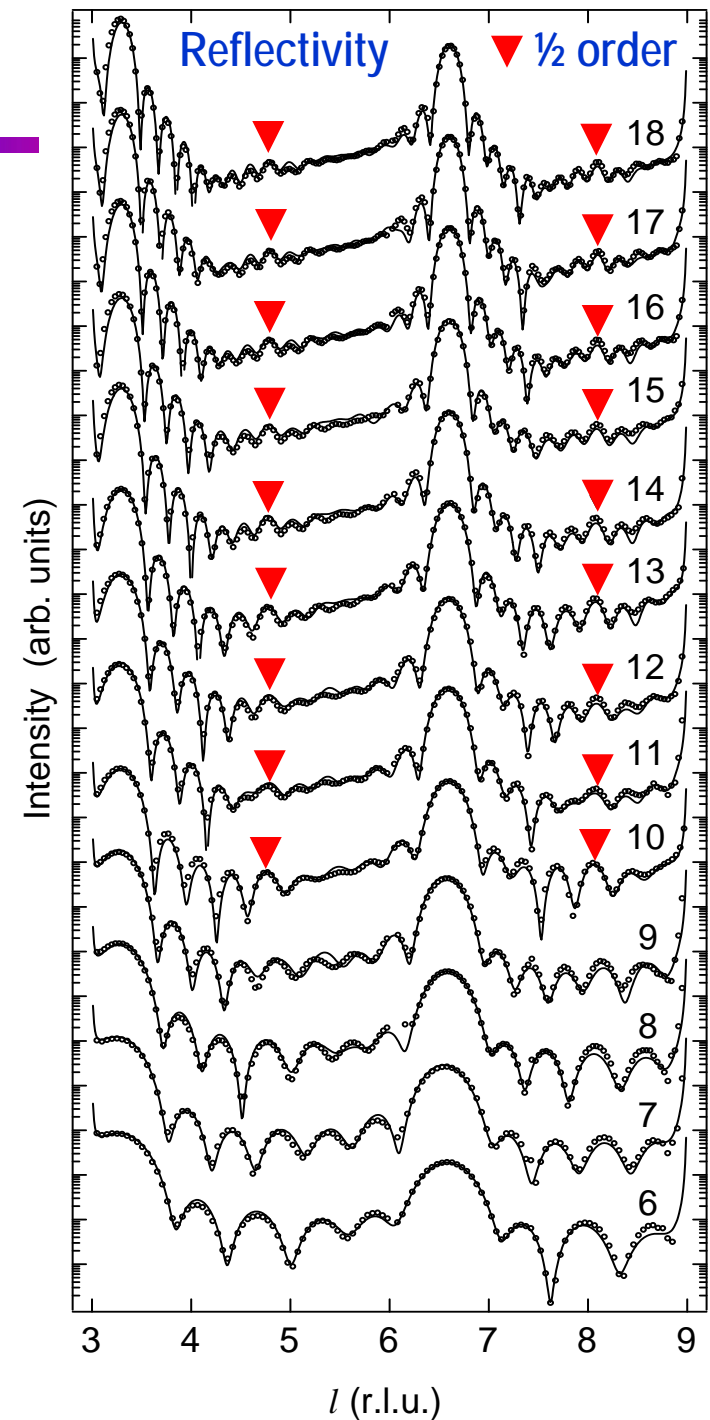
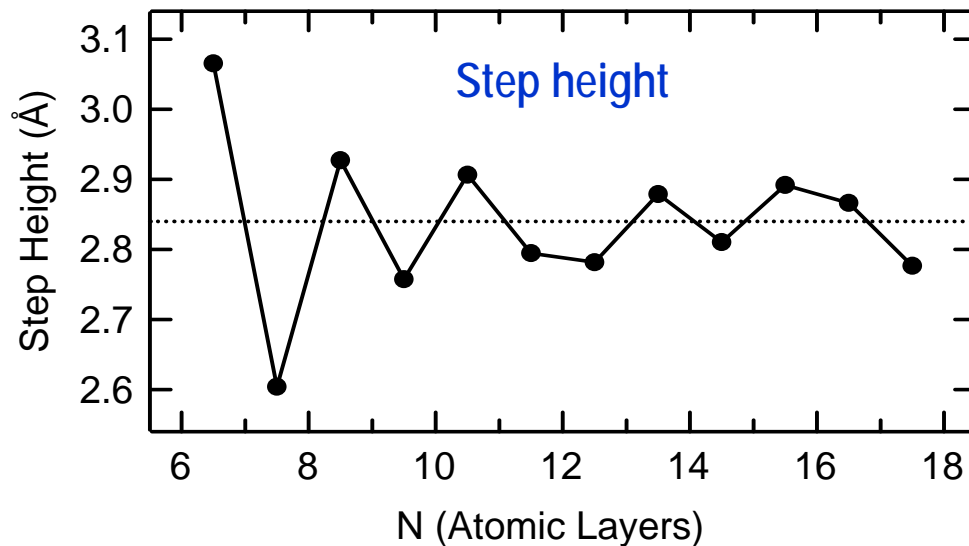
# Charge Oscillations in Real Space

Pb on Pb-terminated Si(111) (root-3 surface)

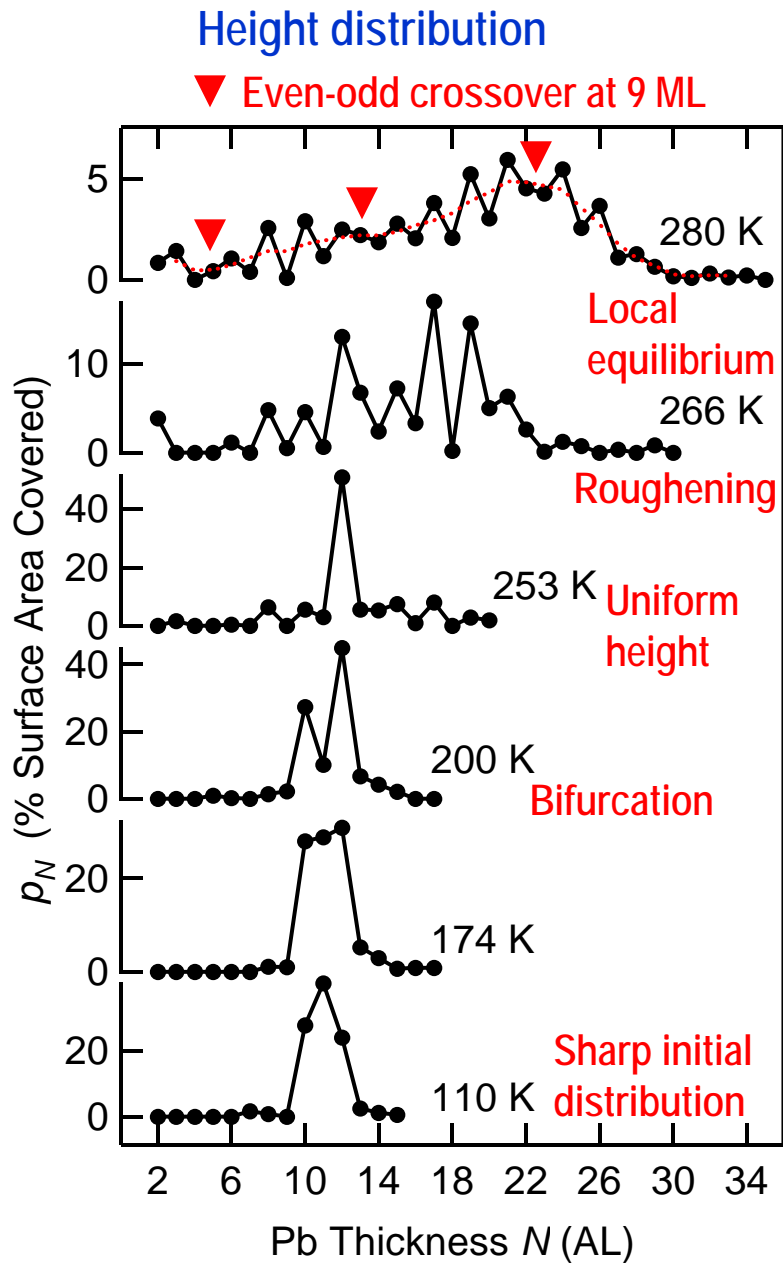
Nearly atomically uniform films (no magic islands)

Half-order peak implies  $\sim 2$  ML modulation

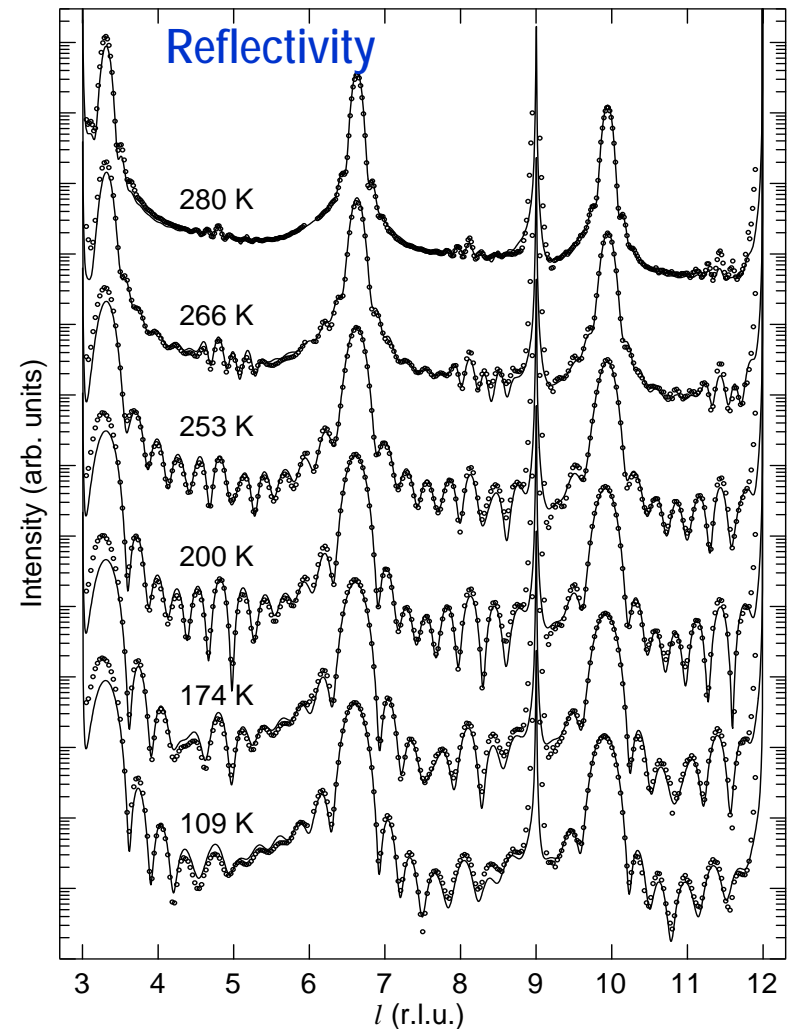
Analysis shows step height oscillations (in agreement with STM and He scattering)



# Direct Measure of Surface Energies



Pb film (11 ML) - annealing spreads out thickness distribution  $\rightarrow$  local thermal equilibrium; bilayer oscillations



## Thickness Dependent Surface Energy

Local thermal equilibrium; fit to free electron results ( $A$  and  $\Delta N$  only)

$$p_N - \frac{p_{N+1} + p_{N-1}}{2} = -\frac{1}{2} p_N''$$

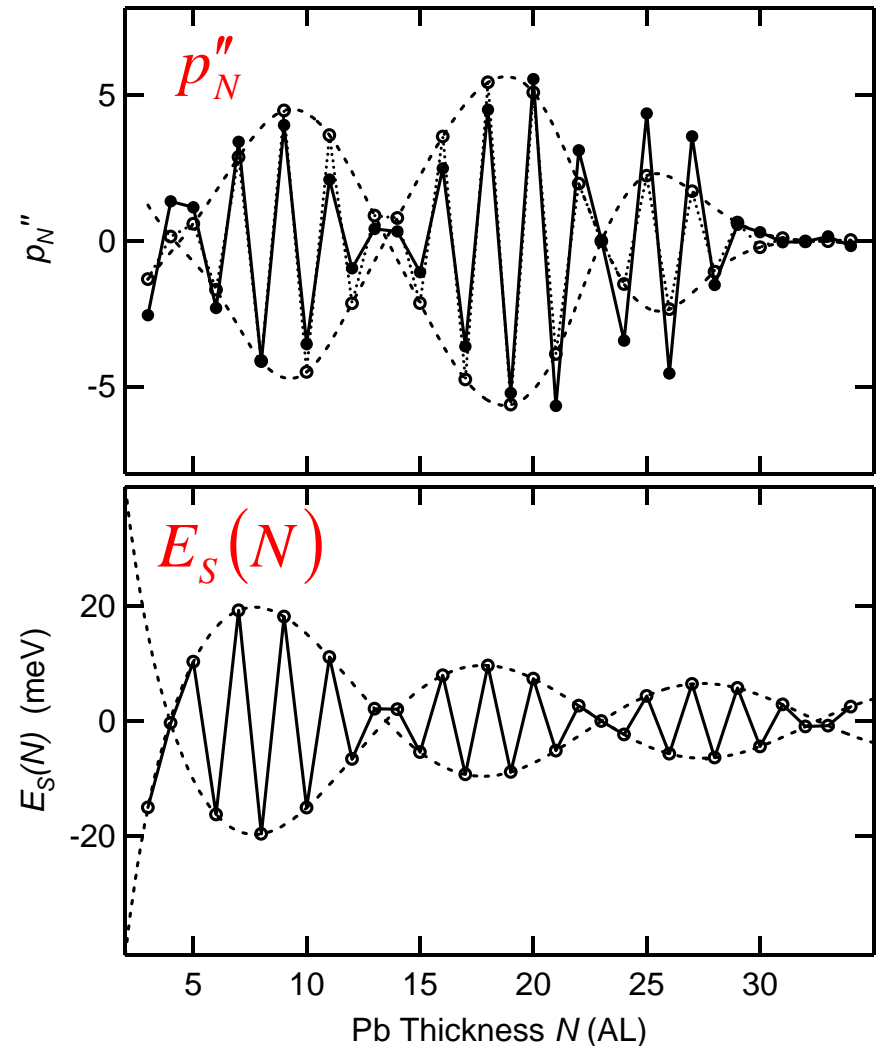
$$p_N \propto \exp\left[\frac{-E_S(N)}{k_B T}\right]$$

$$E_S(N) = A \frac{\cos[2k_F(N + \Delta N)t]}{(N + \Delta N)^\alpha} + B$$

$$\alpha = 0.938$$

$\Delta N$  = charge spillage

Beating between 2.2 & 2 ML yields 9 ML envelope function (even-odd switching)



# Example: TiN Growth on Sapphire by Pulsed Laser Deposition

Anti-Bragg intensity should show bilayer oscillations (contributions from two neighboring layers are out of phase and cancel). Oscillation amplitude = one layer. Oscillations diminish with increasing roughness.

Results show a beating pattern due to non-Gaussian roughness.

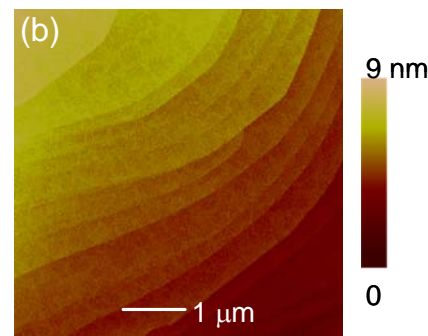
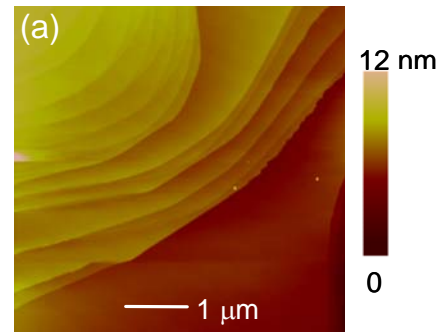
**Amp = 1**

**Amp = 0**

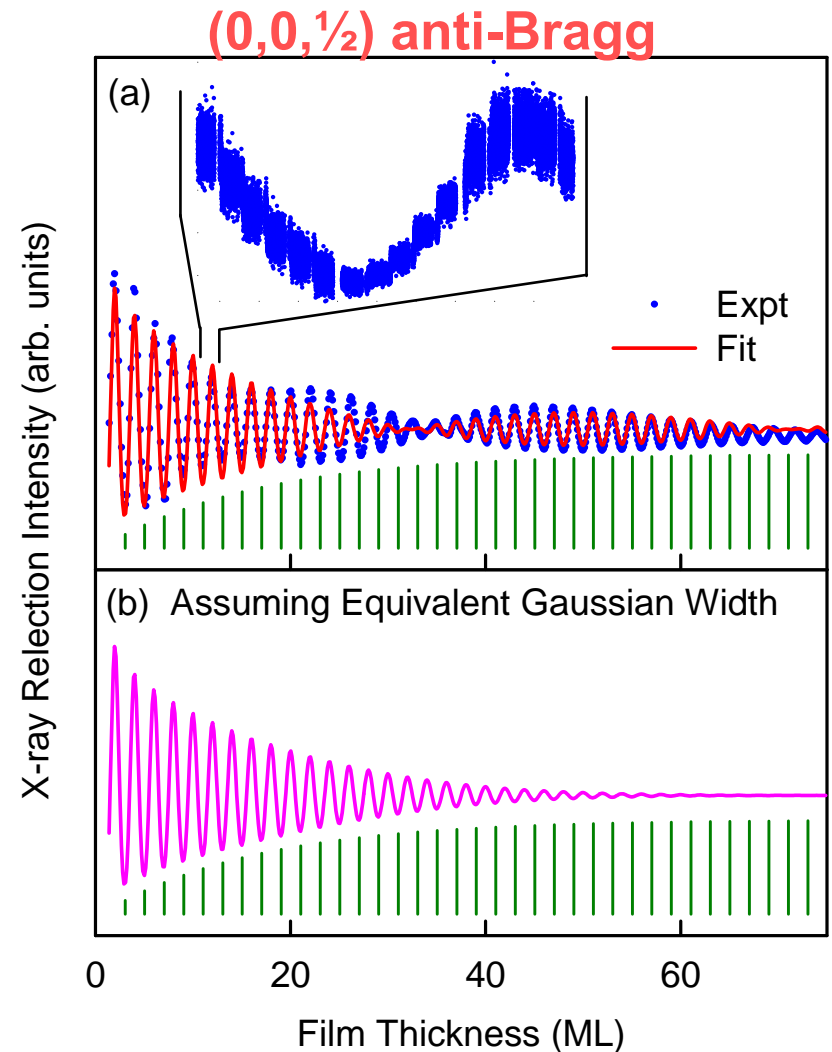
**Amp = 1/3**

**Amp = 0**

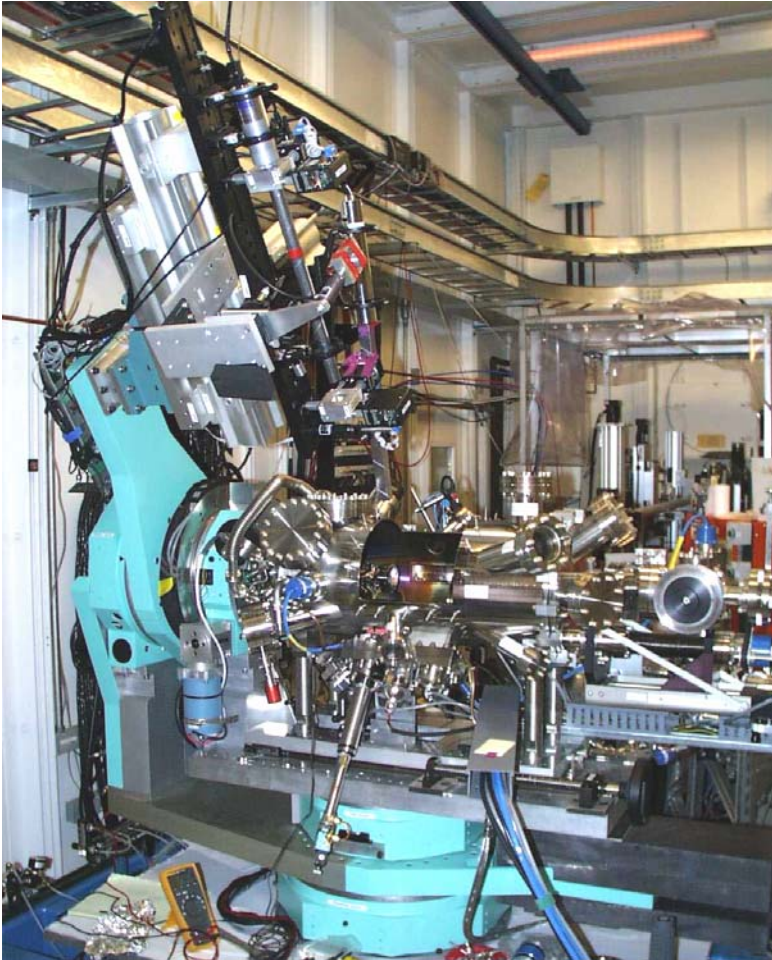
**Etc.**



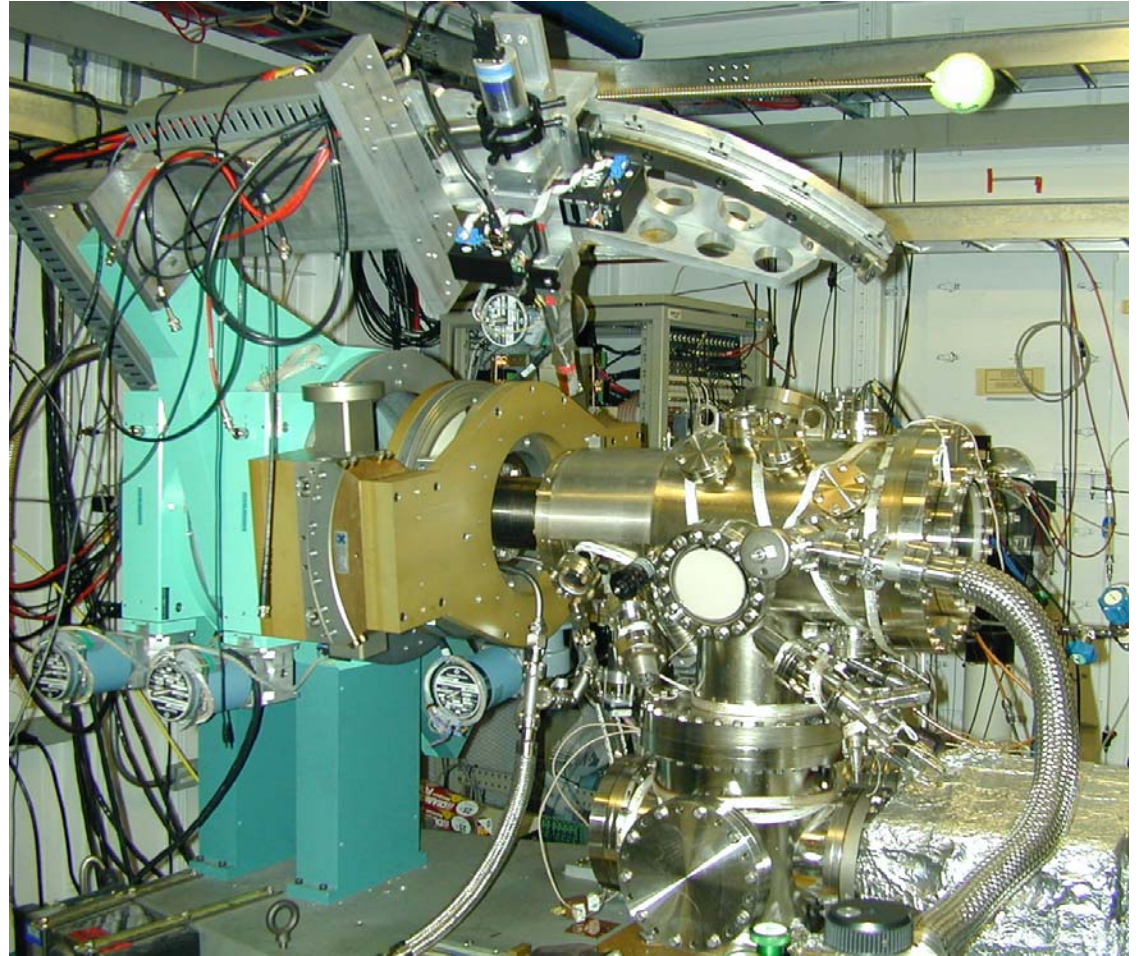
Images before & after growth of 75 monolayers.



## Diffractometers & Vacuum Chambers

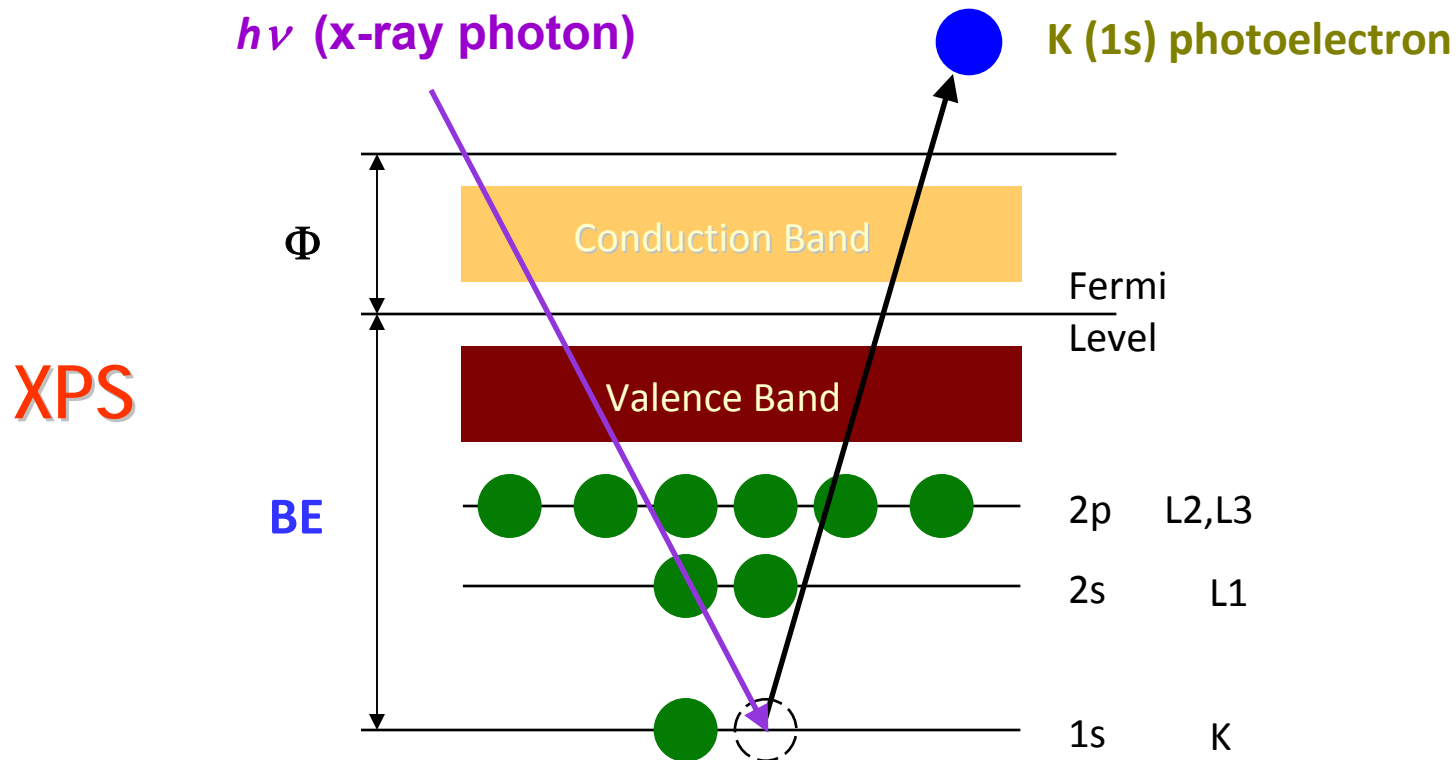


Laser ablation



Molecular Beam Epitaxy

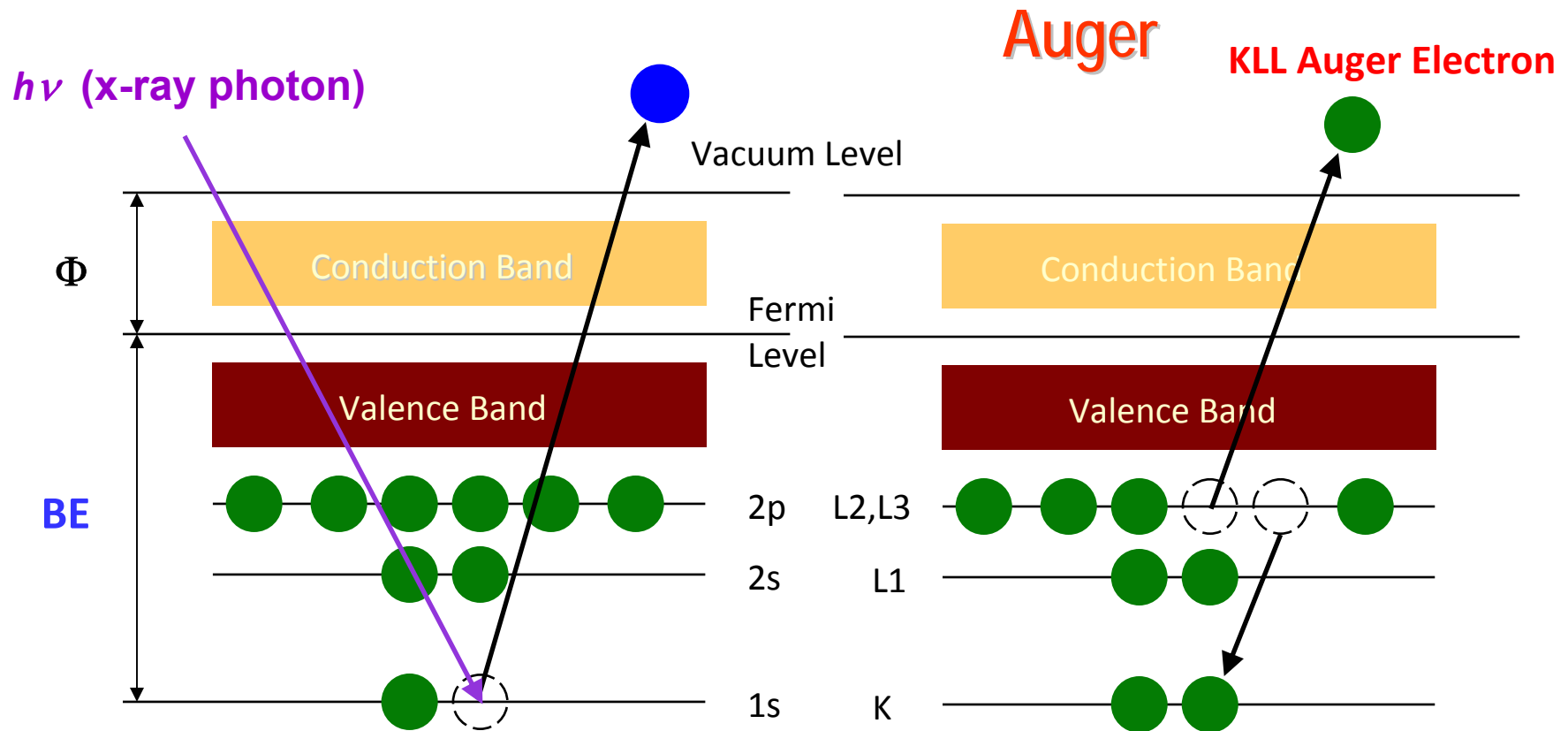
# Surface Spectroscopy – XPS (X-ray Photoelectron Spectroscopy) & Auger



$$\mathbf{KE} \text{ (measured)} = \mathbf{h\nu} \text{ (known)} - \mathbf{BE} - \Phi \text{ (work function)} \quad \mathbf{BE} = \mathbf{h\nu} - \mathbf{KE} - \Phi$$

BE – binding energy depends on  $Z$  (mostly an atomic property). Reference tables available. Fingerprint technique.

Also depends on the chemical state (**chemical shift**;  $\sim 1$  eV for unity increase in oxidation number) and environment (e.g., **surface shift**; typically 0-0.5 eV).



**Core holes** (created by x-ray or electron excitation) decay via two channels:

**X-ray emission or x-ray fluorescence** (more important at high energies)

**Auger decay** is element specific (~atomic effect). Multiplet line shapes and energies provide “fingerprint” identification. Examples: KLL, LMM, MNN, KLM, MMM, ... 2 holes in the final state.

## Mechanism for Auger processes: Coulomb/exchange interactions

$$\left\langle \psi_2' \psi_1' \left| \frac{e^2}{r_{12}} \right| \psi_2 \psi_1 \right\rangle$$

LLM, MMN, ... also known as Coster-Kronig transitions (transitions between same shell). MMM, ... (all three states from the same shell) also known as super Coster-Kronig transitions. CK and super CK are more intense because of better orbital overlap (but usually at low energies).

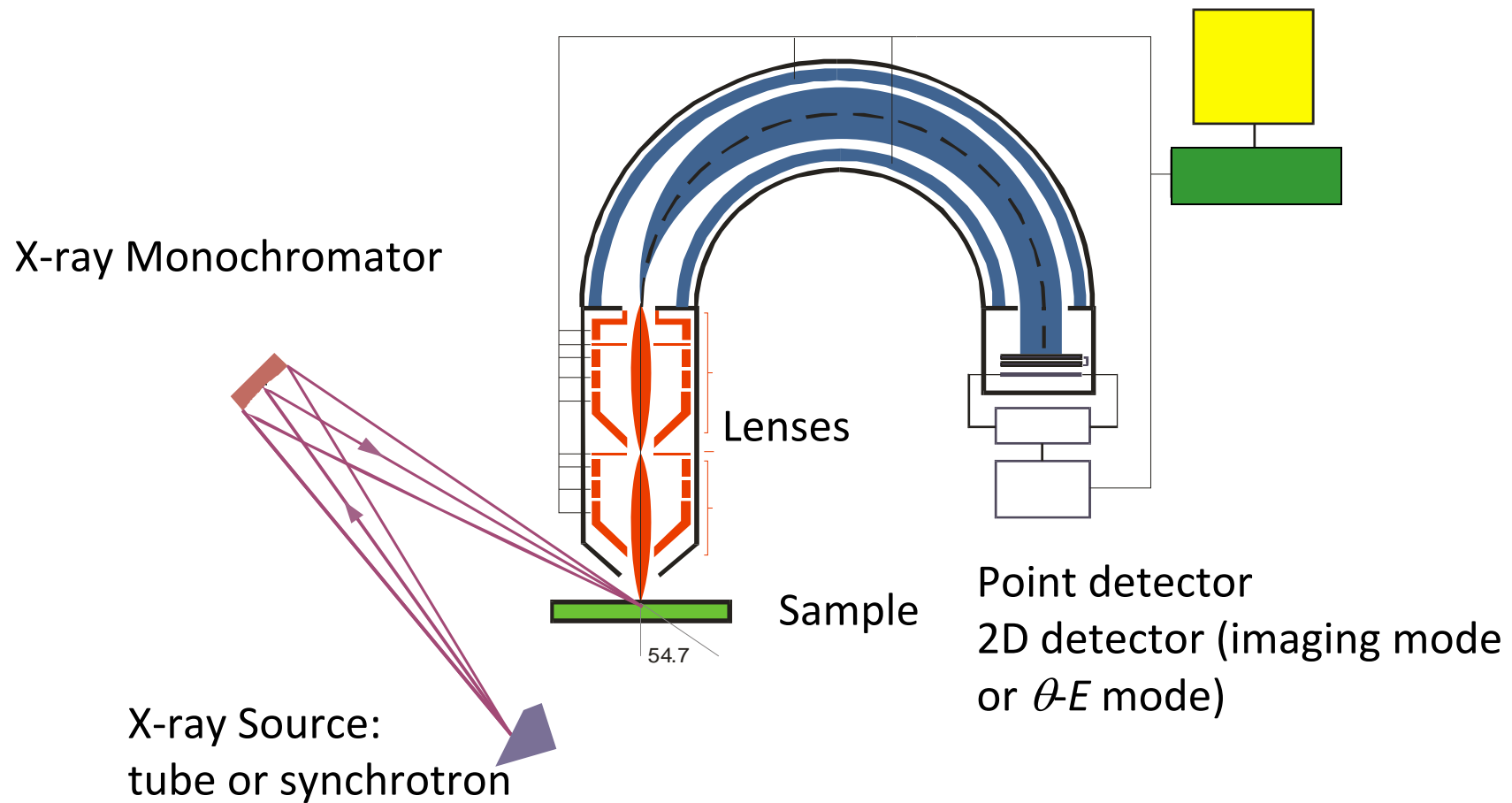
For XPS, the s core levels are singlets; p, d, f core levels are doublets due to **spin-orbit coupling** ( $j = l \pm \frac{1}{2}$ ). The missing electron (hole left behind) has spin  $\frac{1}{2}$ ; it couples with its orbital angular momentum (p, d, and f). Larger splittings for heavier elements.

For Auger, the line shapes can contain multiplets because the spin and orbital angular momenta of the two holes in the final state can couple in different ways.

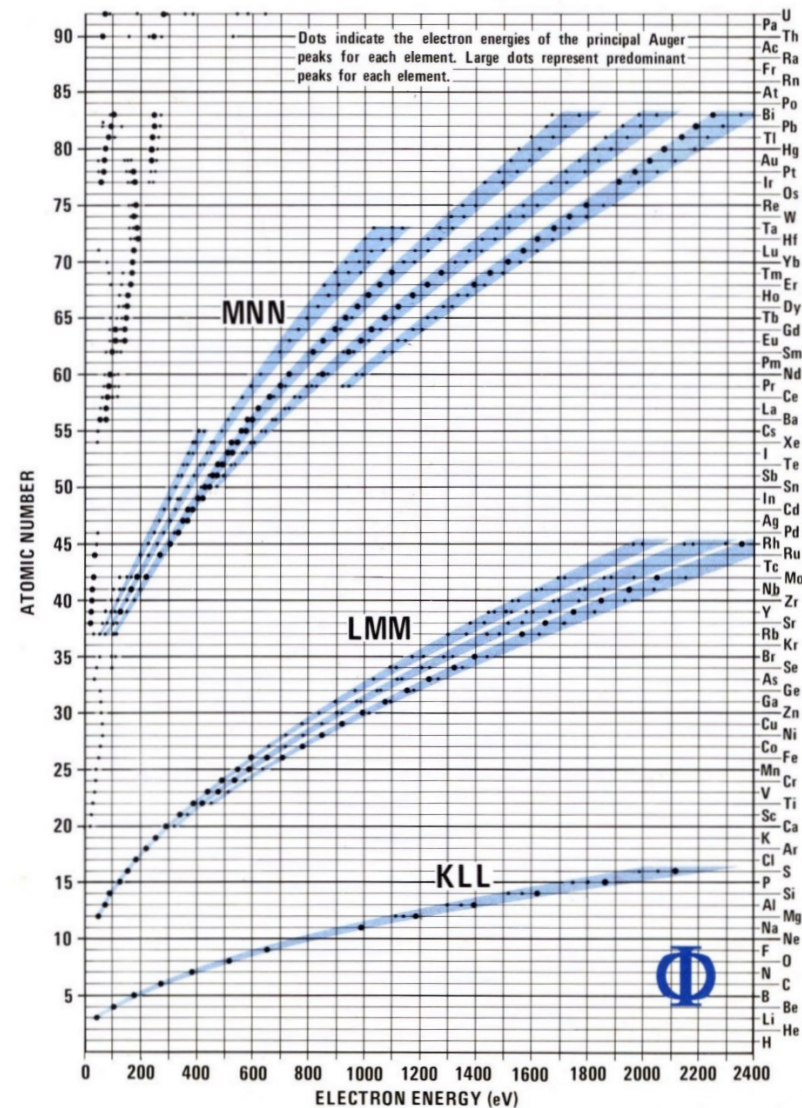
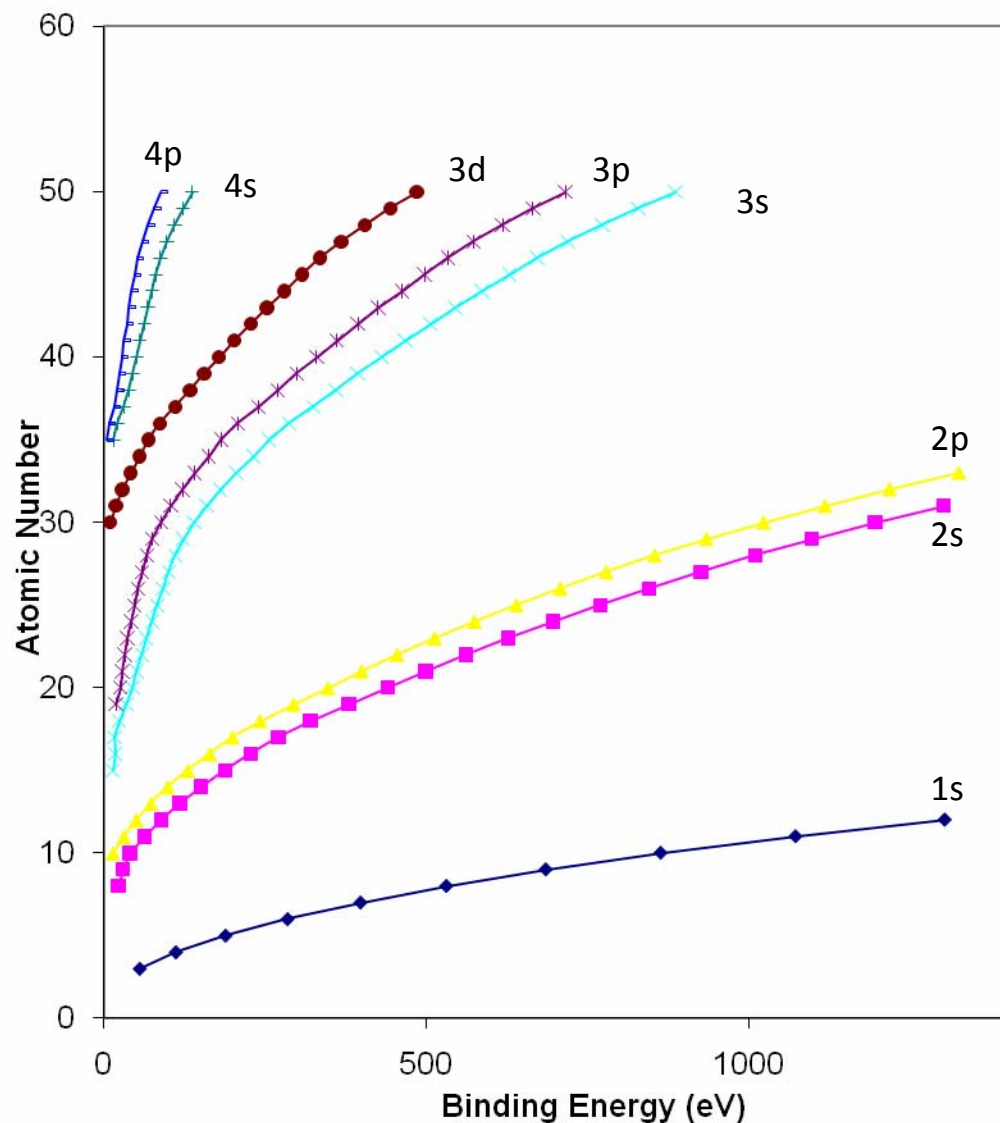
**XPS – at fixed binding energies; Auger – at fixed kinetic energies.** Can be separately identified by varying the photon energy.

# Electron Spectrometers (for detecting XPS and Auger signals)

## Hemispherical Energy Analyzer



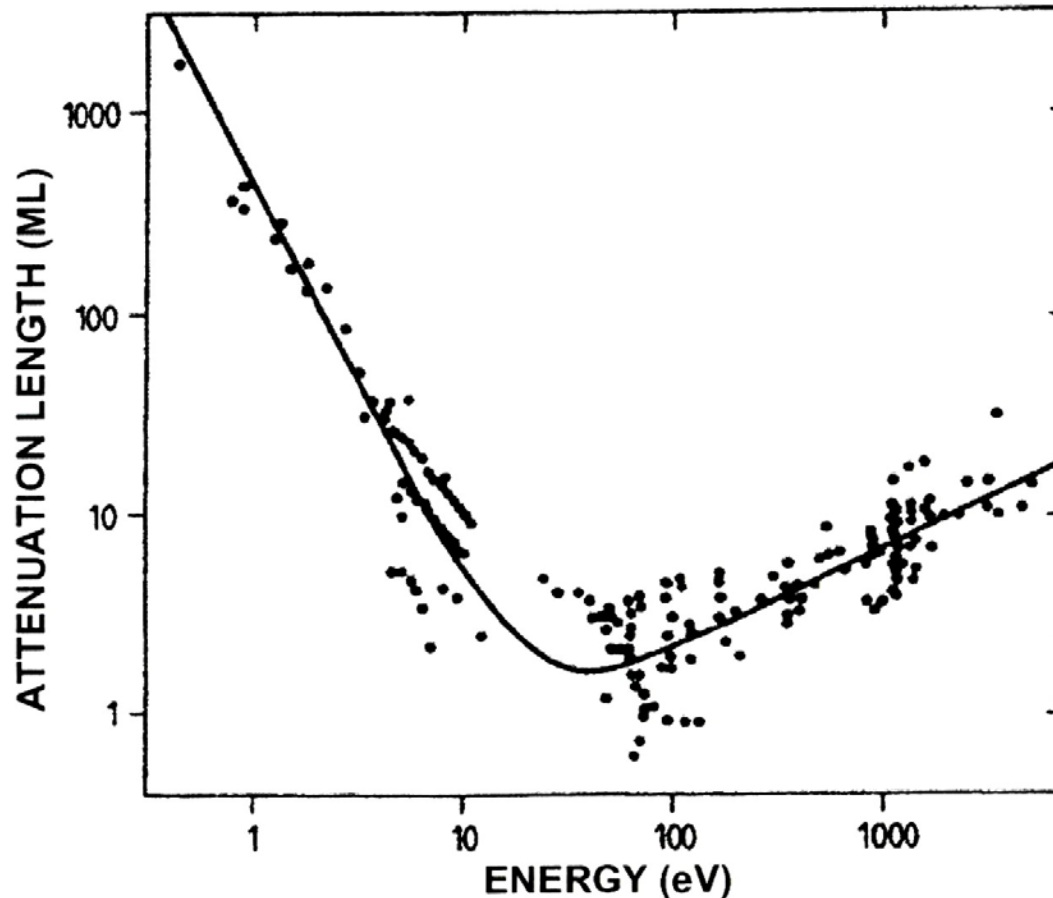
# Core Level Binding Energies & Auger Kinetic Energies



Energies and line shapes – fingerprints.

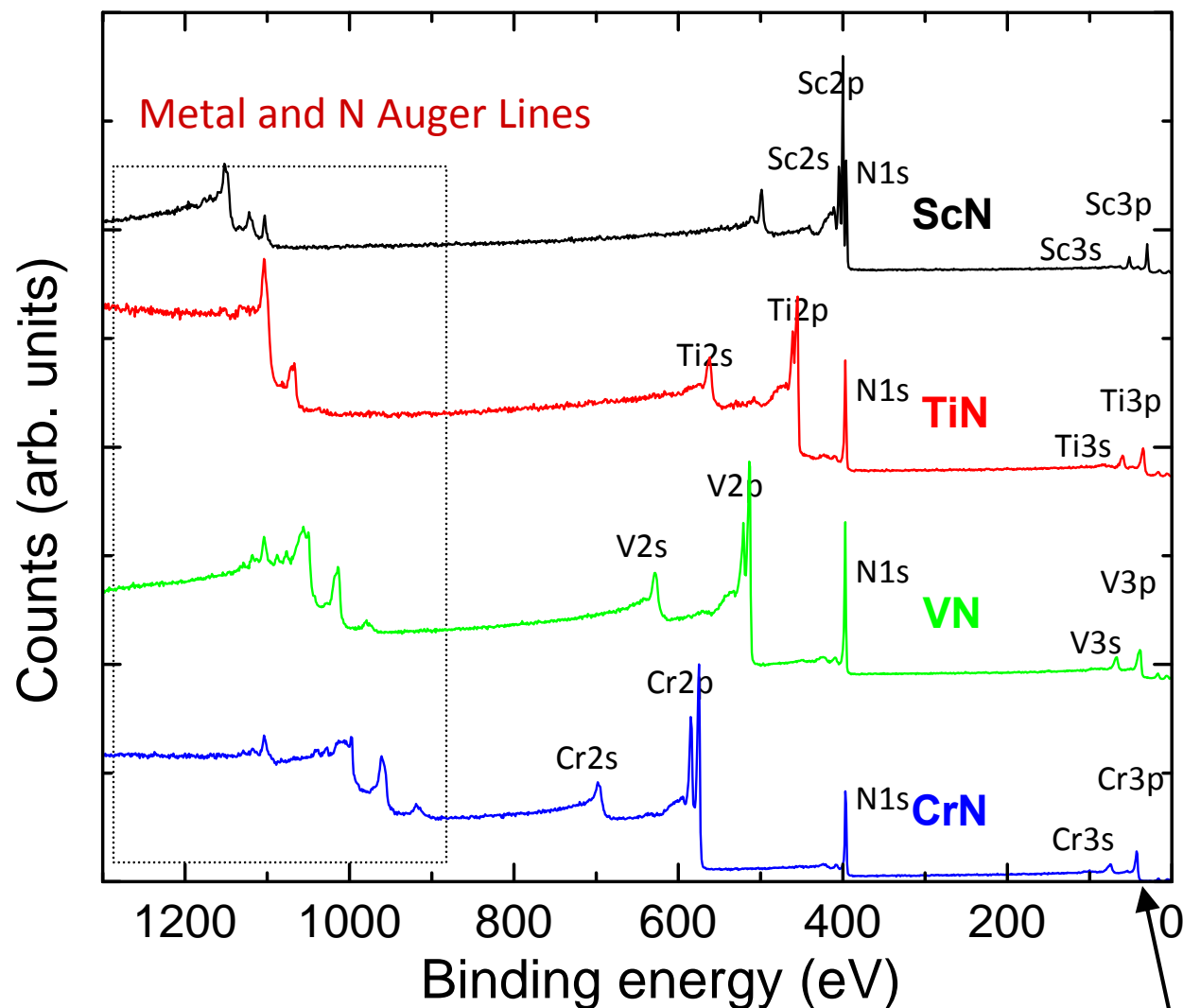
L. E. Davis, N. C. MacDonald, Paul W. Palmberg, G. E. Riach, R. E. Weber, *Handbook of Auger Electron Spectroscopy*, 2<sup>nd</sup> Edition, Physical Electronics Division, Perkin-Elmer Corp., Eden Prairie, MN 1976.

## High Surface Sensitivity (due to a short mean free path of the electrons)



Short mean free path  $\sim 4\text{-}20 \text{ \AA}$  caused by scattering by electrons, plasmons, & phonons. Phonon scattering is important at very low energies while electron scattering diminishes due to a reduced phase space. M. P. Seah & W. A. Dench, *Surf. Interf. Anal.* **1**, 2 (1979).

# Examples of XPS and Auger Spectra



s levels – one peak

p levels – two peaks  
(spin-orbit splitting)

Auger – multiplet  
splittings

Step-like increases in  
background from  
inelastic scattering

Bulk and surface  
plasmon satellites

XPS peaks could be  
asymmetric because of  
low energy electron  
excitations.

3p valence bands

# XPS from Valence Bands – Density of States

Background subtracted XPS spectrum of GaP

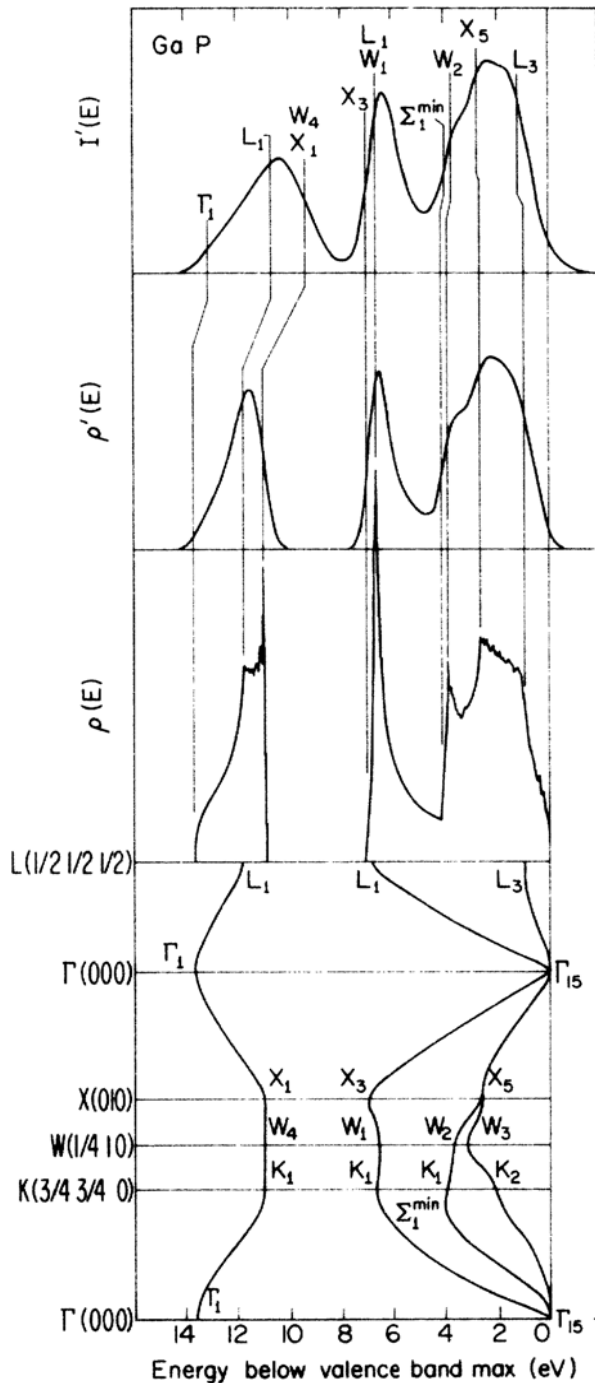
Broadened DOS (lifetime effects)

DOS (density of states)

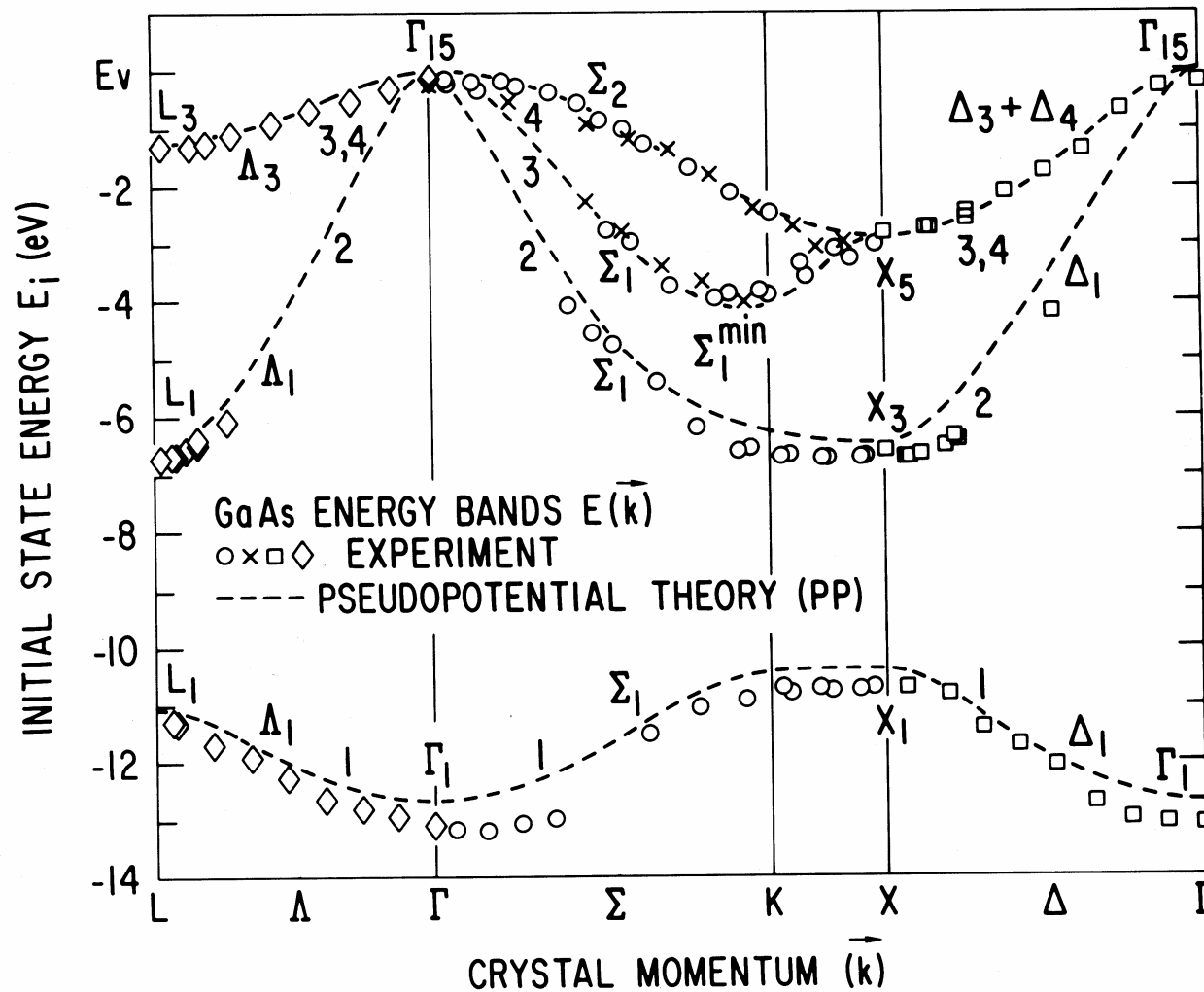
L. Ley, R.A. Dollack, F.R. McFeely, G. P. Kowalczyk, and D.A. Shirley, Phys. Rev. B **9**, 600 (1974).

Band structure of GaP

Ideally, one wants to map the bands – can be done with angle-resolved photoemission.

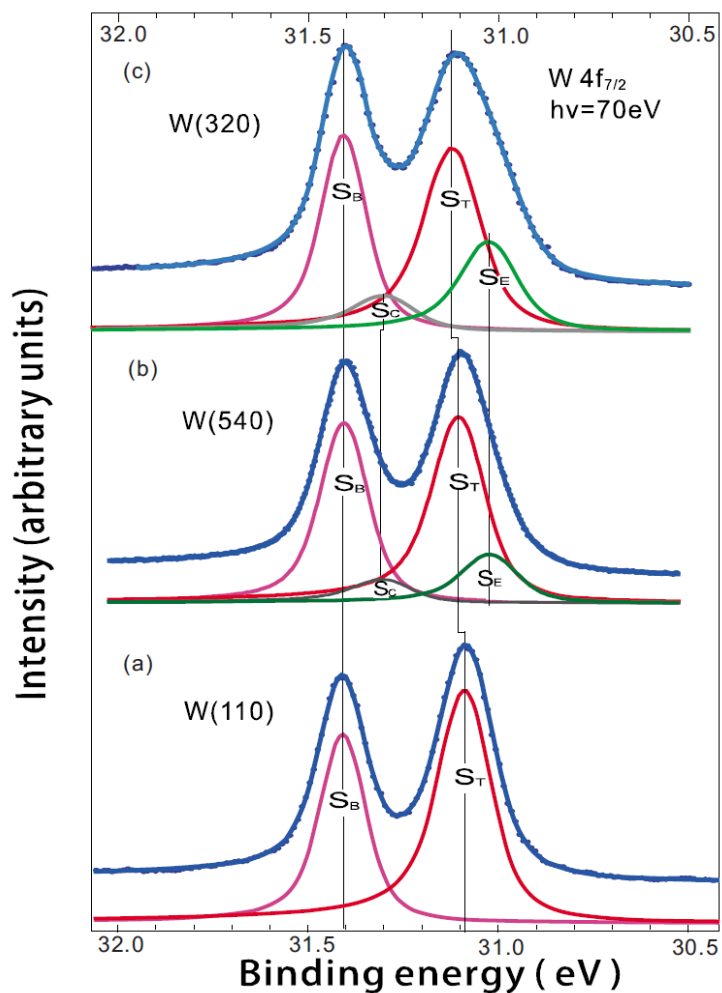


## Example: Band Mapping by Angle-Resolved Photoemission

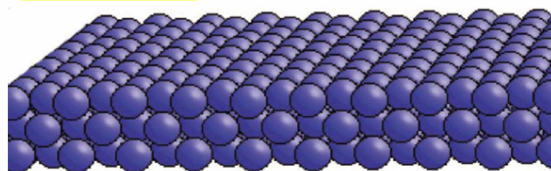


APS is developing a beamline for high-energy angle-resolved photoemission: higher bulk sensitivity useful for separating out surface effects.

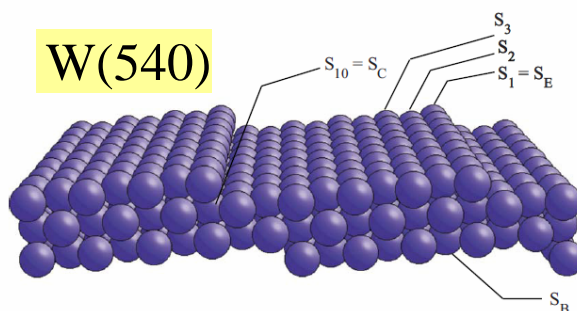
# Example: Surface Core Level Shifts of W $4f_{7/2}$



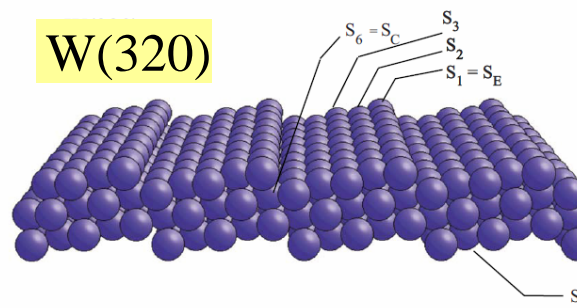
W(110)



W(540)



W(320)



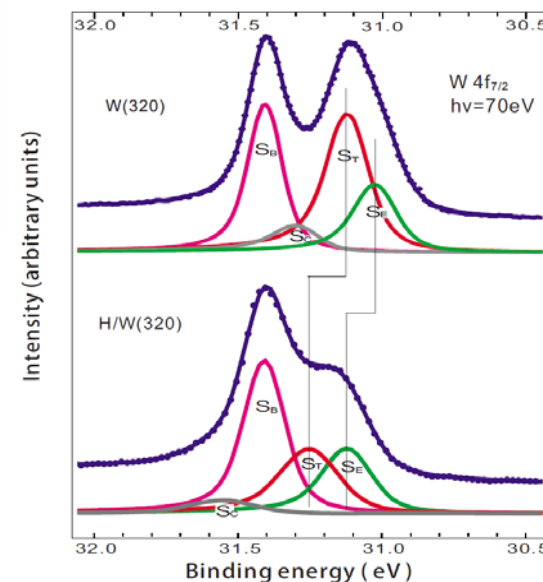
$S_B$  = bulk

$S_T$  = terrace

$S_C$  = corner

$S_E$  = step edge

H-induced  
chemical shifts  
(charge transfer)

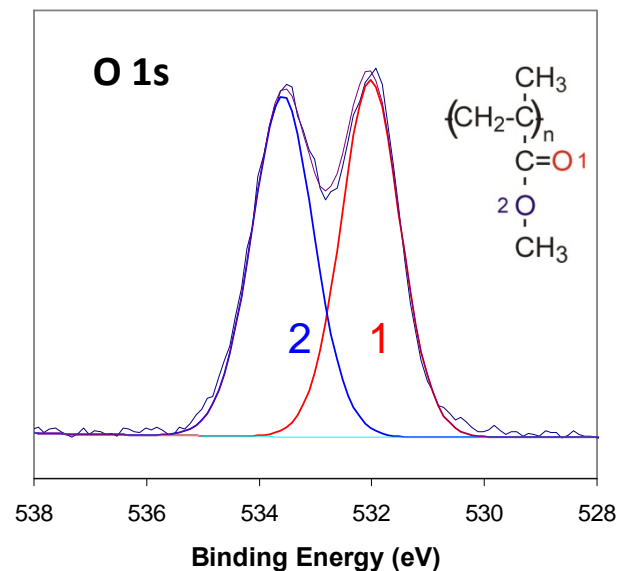


$4f_{5/2}$  not shown. Surface shifts are usually small, 0 – 0.5 eV. Can be related to surface electronic structure. X. Zhou and J. L. Erskine, Phys. Rev. B **79**, 155422 (2009).

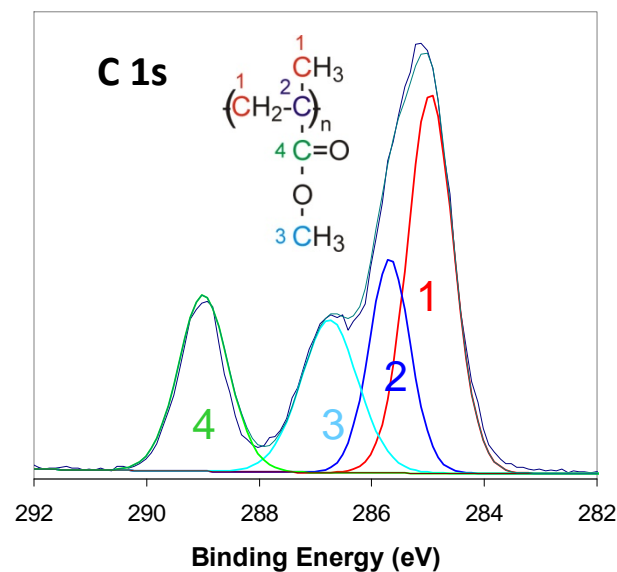
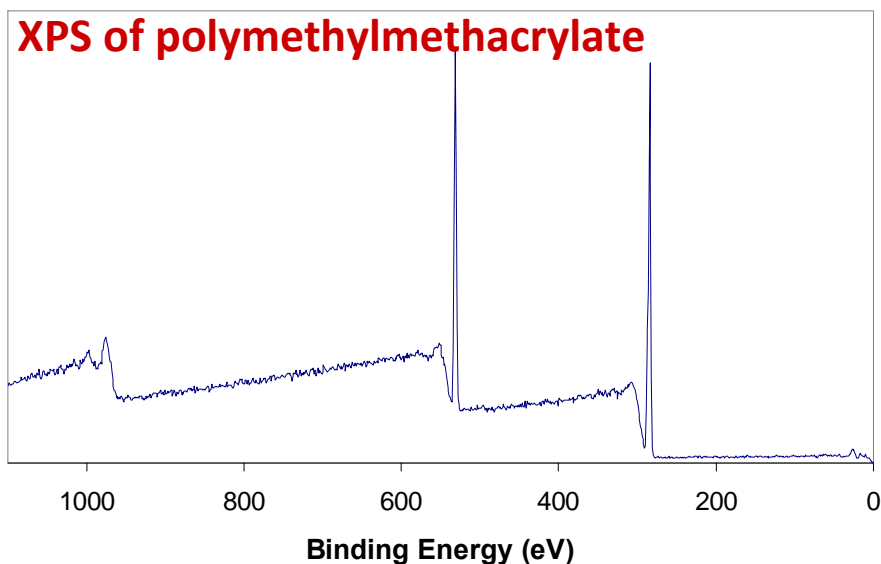
# Chemical Shifts (useful for identifying chemical states)

Core level binding energies depend on chemical bonding (charge transfer).

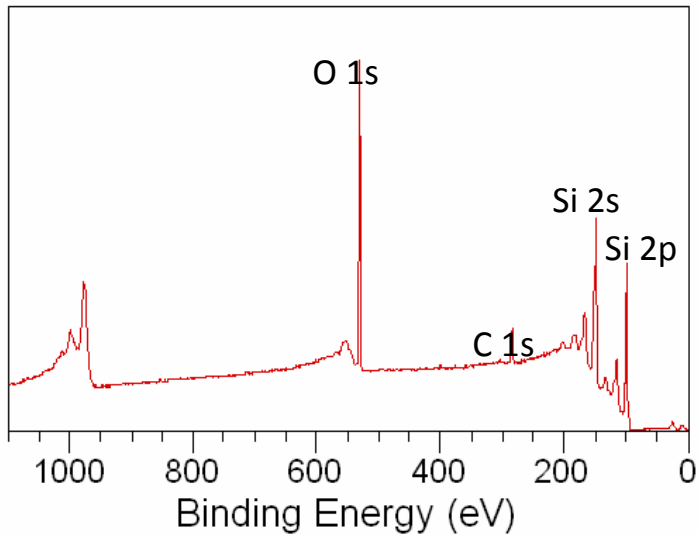
Functional Group		C 1s Binding Energy (eV)
hydrocarbon	<u>C</u> -H, <u>C</u> -C	285.0
amine	<u>C</u> -N	286.0
alcohol, ether	<u>C</u> -O-H, <u>C</u> -O-C	286.5
Cl bound to C	<u>C</u> -Cl	286.5
F bound to C	<u>C</u> -F	287.8
carbonyl	<u>C</u> =O	288.0



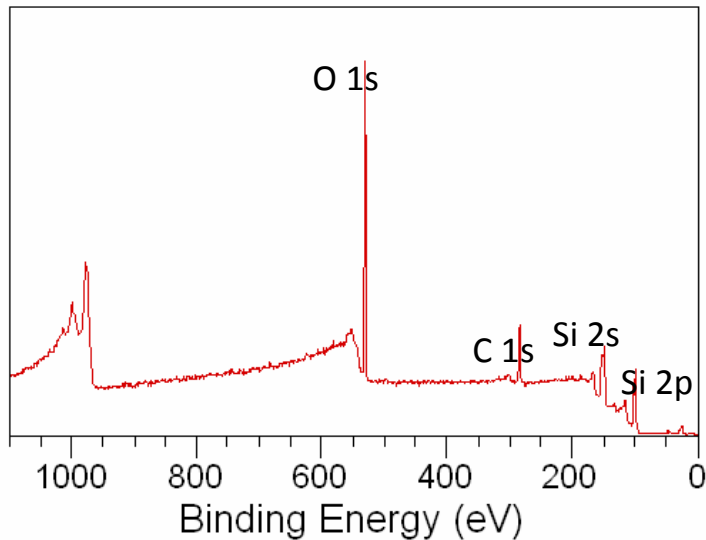
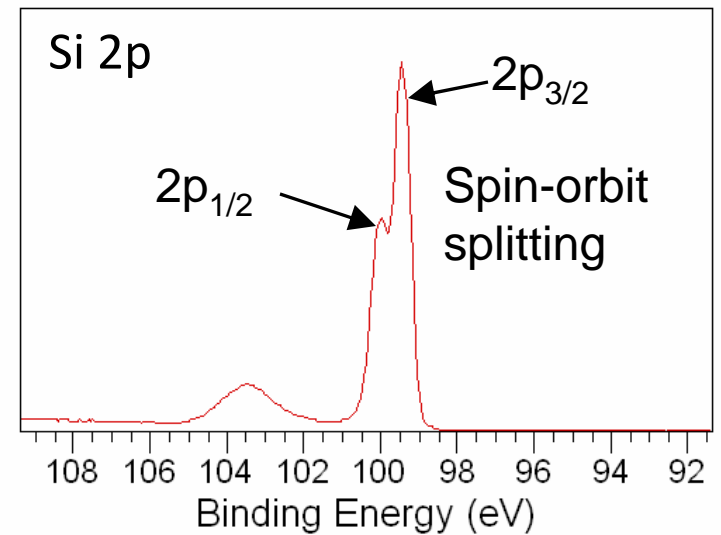
## XPS of polymethylmethacrylate



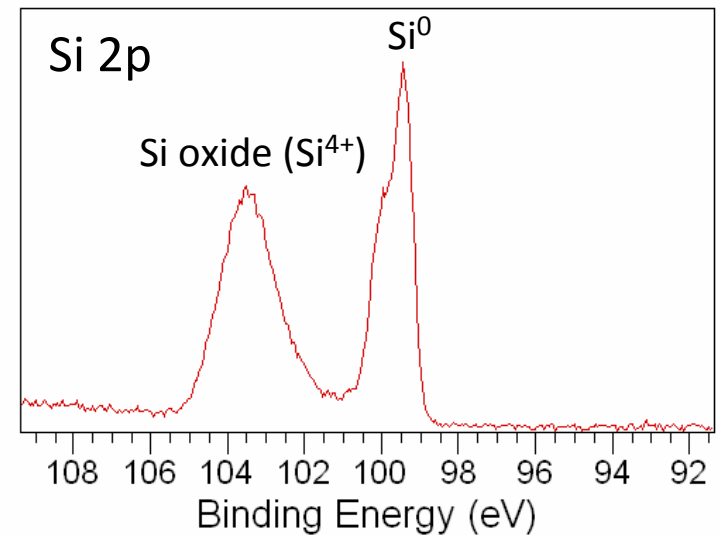
## Example: Angle-Resolved XPS from Si with Native Oxide



$\theta = 0^\circ$



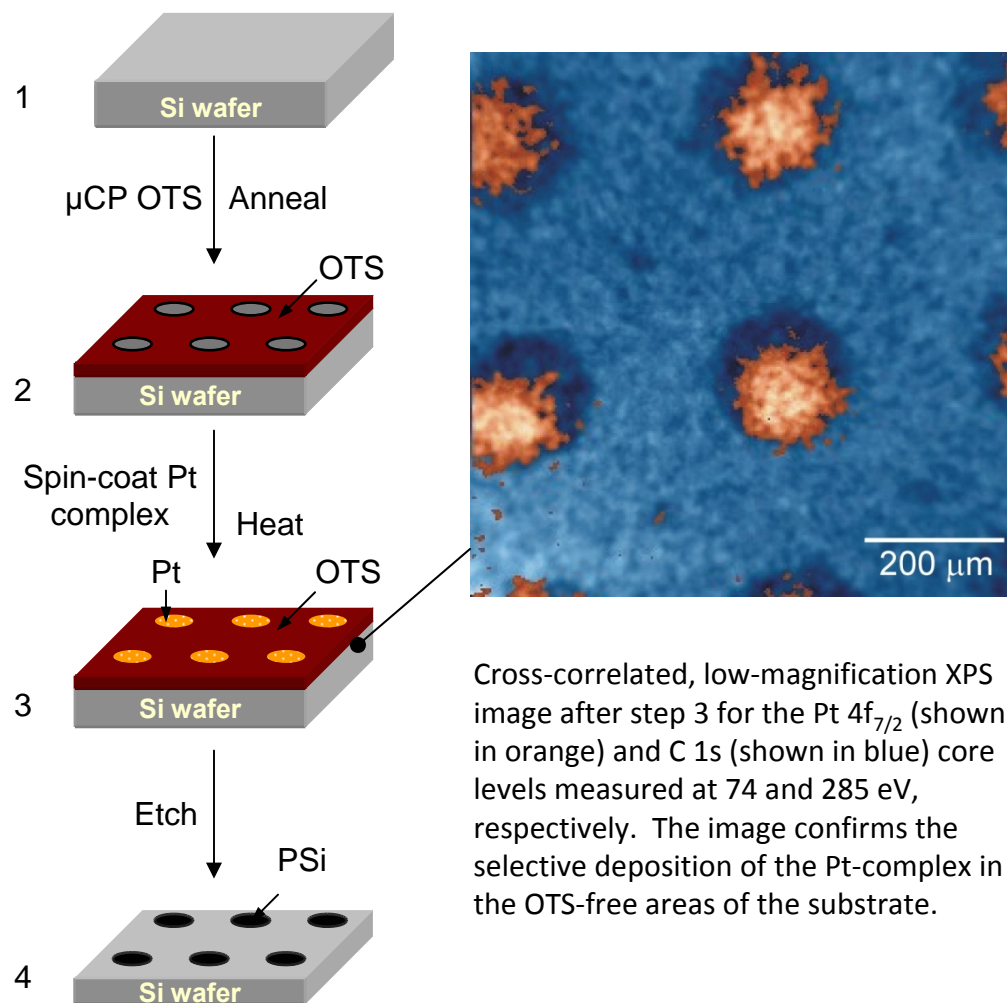
$\theta = 75^\circ$   
grazing, more surface sensitive



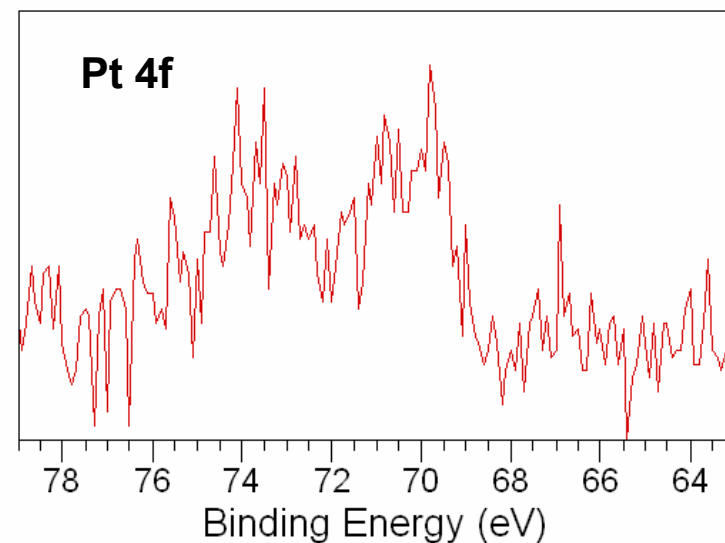
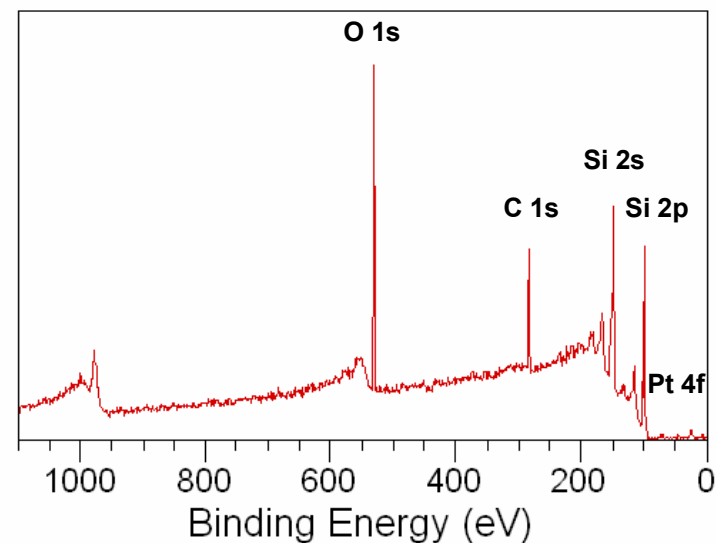
A more positive chemical state (e.g.,  $\text{Si}^{4+}$ ) has a higher binding energy: the outgoing photoelectron is “slowed down” by the Coulomb attraction – lower KE.

# Example: XPS Imaging (Chemical Mapping)

## Pt catalyzed etching of patterned porous silicon

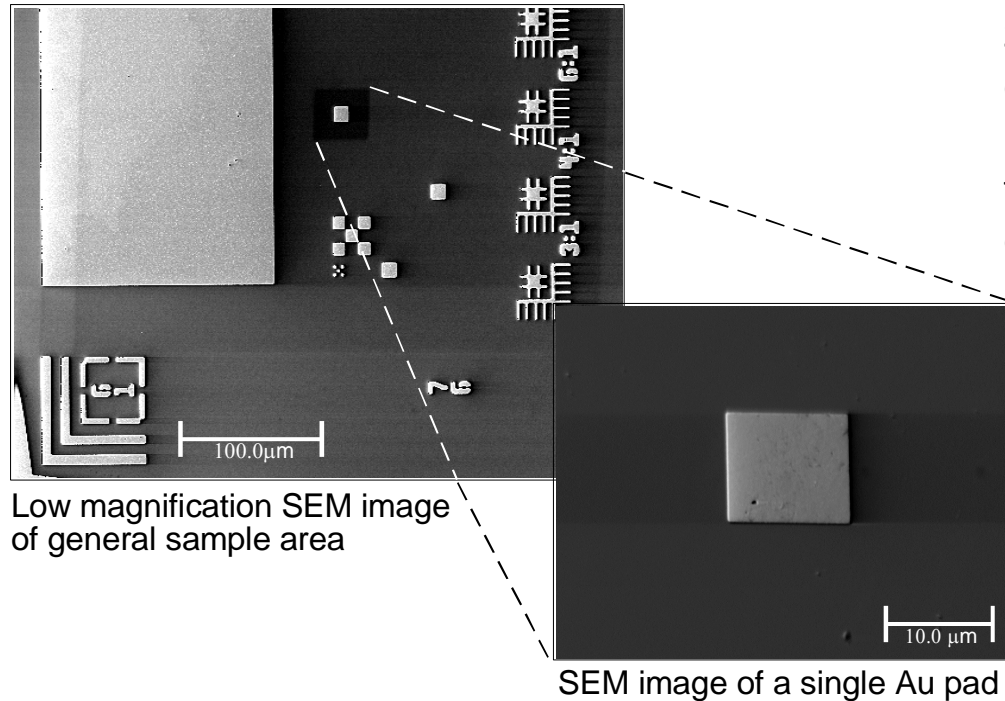


Cross-correlated, low-magnification XPS image after step 3 for the Pt  $4f_{7/2}$  (shown in orange) and C  $1s$  (shown in blue) core levels measured at 74 and 285 eV, respectively. The image confirms the selective deposition of the Pt-complex in the OTS-free areas of the substrate.

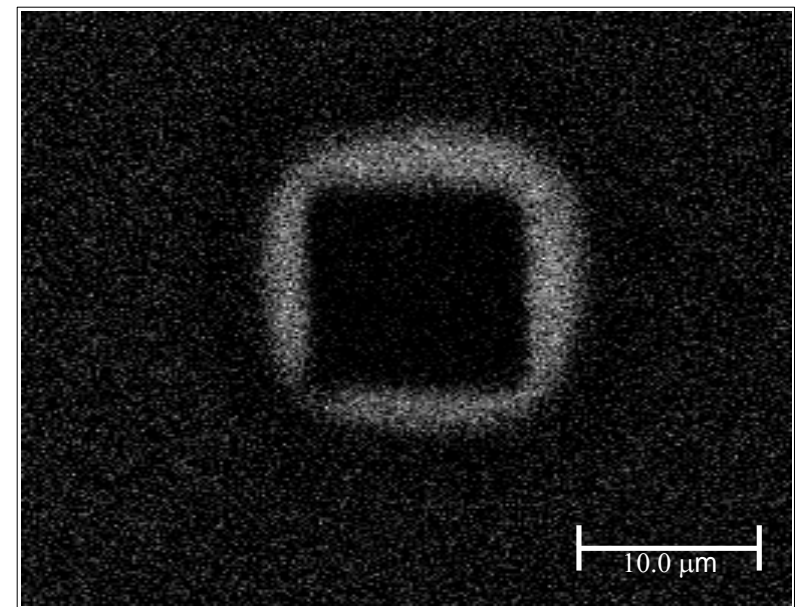


# Example: Auger Imaging (Chemical Mapping)

## Contamination on patterned semiconductor



Survey data was used to identify Indium (In) contamination after the etching step on a patterned semiconductor. Then mapping of the In signal showed the position of contamination on the sample.



## Some Future Directions for Surface X-ray Scattering

---

Direct methods of structural determination (without assumed models & fitting)

X-ray phase determination

Coherent diffraction methods

Small probe spots for local analysis of nanostructures

Dynamics

Extreme conditions ( $T$ ,  $p$ ,  $B$ ,  $E$ , etc.)

In-situ surface, thin film, and nanostructure processing

Simultaneous property measurements (such as transport)

## Acknowledgments

---

Some of the XPS/Auger slides are from Rick Haasch (FSMRL, UIUC).